This is to certify that the
thesis entitled

Fault Types and Reliability Estimates in Permanent Magnet
AC Motors

presented by

John David Neely

has been accepted towards fulfillment
of the requirements for the

M.S. degree in Electrical Engineering

EG Strangas

Major Professor's Signature

05/02/2005

Date

Fault Types and Reliability Estimates in Permanent Magnet AC Motors

By

John David Neely

A THESIS

Submitted to
Michigan State University
in partial fulfillment of the requirements
for the degree of

MASTER OF SCIENCE

Department of Electrical and Computer Engineering

2005

ABSTRACT

Fault Types and Reliability Estimates in Permanent Magnet AC Motors

By

John David Neely

The ability to detect and mitigate a fault is critical for electrical drives and machines in applications that require high reliability. In this work, a Permanent Magnet AC drive and machine is examined and the most critical areas are analyzed for reliability. An algorithm is provided to determine the reliability of a drive and motor. Remedial designs are also consider for either mitigating a fault or producing a fault tolerant design. An analysis is performed to determine the reliability when remedial solutions are employed.

To my parents, Richard and Rita

ACKNOWLEDGMENTS

I would like to express my gratitude and thanks to my thesis advisor Professor Elias Strangas for his guidance, support, and his professional as well as personal example. I would also like to thank Professors Robert Schlueter and Fang Peng for their time and effort in being part of my committee. I would like to extend special thanks to the Division of Engineering Computing Services and their Director, Jackie Carlson, for providing funding for graduate school. Special words of thanks go to my lab colleagues Wes Zanardelli and Sinisa Jurkovic. Finally, I owe special thanks to my parents, Richard and Rita Neely, whose support and encouragement helped make my graduate studies possible.

TABLE OF CONTENTS

LIST OF TABLES

LIST OF FIGURES

CHAPTER 1

Introduction

Since the invention of AC electrical motors, they have changed greatly. Early motors were single phase and could only provide a constant speed from a given voltage supply. Recent advances in technology have allowed for more advanced designs that utilize three phases to provide variable speed and torque. The use of inverters to control three phase motors allows for a greater versatility in the application of motors. Three phase permanent magnet AC (PMAC) motors offer variable speed and torque control through the use of an inverter. In Figure 1.1, the inverter converts DC voltage into three equal amplitude sinusoidal AC waves using Pulse Width Modulation (PWM). The electrical drive (or controller) is comprised of two main components: a DSP or microprocessor and switches (MOSFETS or IGBTs) of the inverter. The microprocessor runs the necessary software program to determine the PWM, which drives the switches on and off to create a three phase source.

As drives and motors become more complex, the probability of failure increases. In certain applications, a failure is not acceptable and may cause lose of human life or lead to unacceptable downtime. Advances in motor and controller design have led to the ability to detect faults as they occur, and to mitigate the fault keeping the motor running at a reduced performance level that can continue operation. However, depending on the fault correction used, unwanted or unforseen side effects can occur that may cause additional failures in the motor and controller. Understanding the reliability of a motor and its controller before and after a fault allows for better decisions before putting a motor and controller into use.

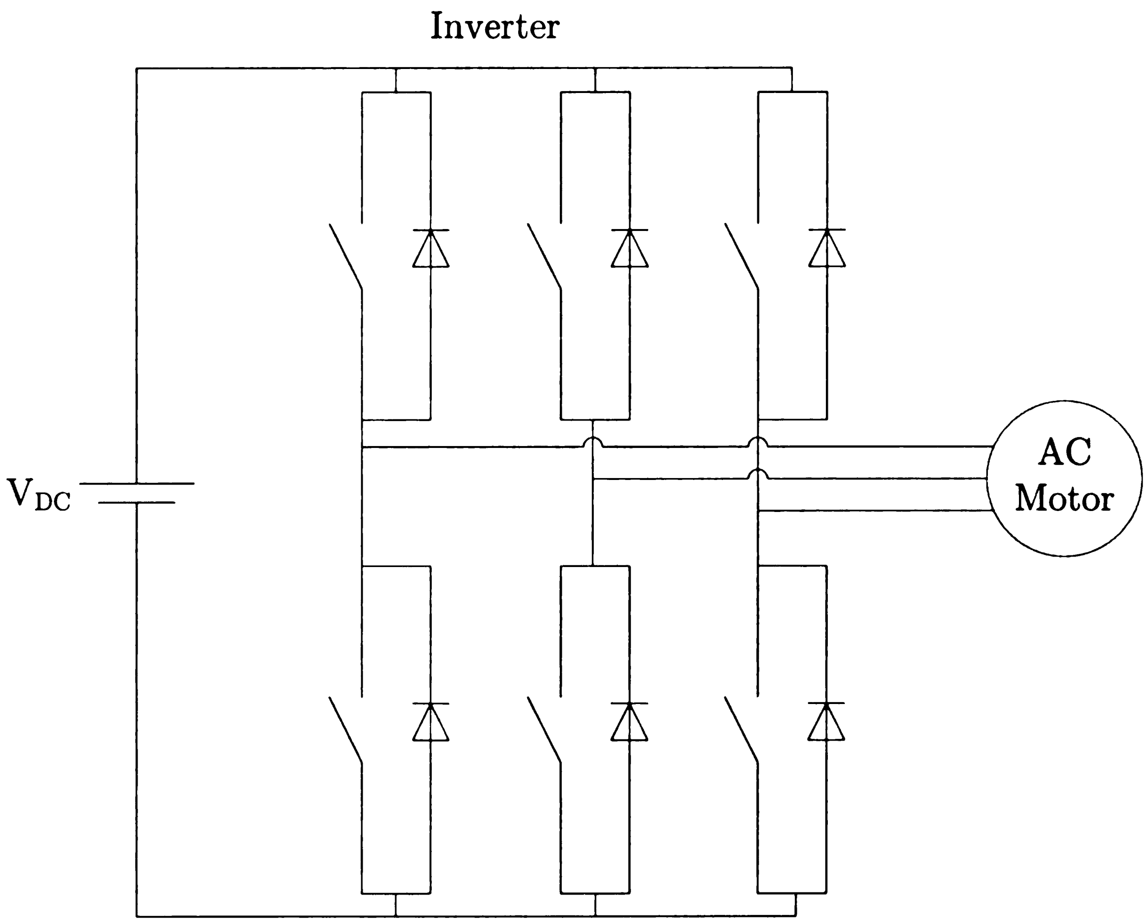

Figure 1.1. Standard Three Phase AC Motor System

Fault detection and mitigation are critical in drives and motors that require a high reliability in applications like steer–by–wire. There are numerous possible faults that could occur during operation. Symptoms of a fault include high currents, torque pulsation, increased temperatures, and fluctuations in voltage. The ability to detect and recover from such faults is important to maintaining a reliable system for a critical application. In the case of automotive steer–by–wire, it would be unacceptable and dangerous to the driver if the steering motor failed and the driver lost control of the vehicle. A more reasonable case would allow the system to detect a drive fault and take the necessary actions to correct the fault, avoiding a failure. All this would be invisible to the driver, with the exception of the dashboard light signaling to have system maintenance performed.

The purpose of this thesis is to lay the ground work to provide a fundamental understanding of faults, mitigation, and reliability in electrical machines. Mitigation solutions are provided based on previous work, and an analysis is performed to show how mitigation will affect a drive and motor after a fault. Algorithms are provided to show how reliability can be predicted given the mode of failure. Examples for the center tapped DC-bus and redundant hardware mitigation techniques are presented and analyzed using the reliability algorithms.

CHAPTER 2

Modes of Failure

There are several key components of a PMAC drive and motor that, when one of them fails, the result is total motor failure. For a permanent magnet AC motor, these components are semiconductors, winding insulation, permanent magnets, and shaft bearings. In works published by P.H. Mellor *et al.* and B.C. Mecrow *et al.*, the two basic faults are open circuit and short circuit [MAOR03], [MJHC96]. These basic faults can occur at the phases of the motor, including both the electronics on the controller and the windings of the motor. The other areas that are susceptible to faults are the permanent magnets and shaft bearings. These faults can be a secondary phenomena resulting from either an open or short fault occurring first. The first step is to identify an open and short fault, then investigate how magnets and bearings can become damaged.

2.1 Primary Faults

2.1.1 Open Circuit Faults

An open circuit fault occurs in one of the motor phases in either the drive or the motor itself. A single switch can fail in the controller, causing either the positive or negative DC bus to be disconnected, as in Figure 2.1 (a). Alternatively, both switches in a phase can fail causing the entire phase to be disconnected from the DC bus, as seen in Figure 2.1 (b). Inside the motor, the stator winding can break, causing the phase to open. In any of these cases, the phase will appear disconnected or open circuited. No fault three phase voltage and current can be seen in Figure 2.2 (a) and Figure 2.2 (b), respectively, and is characterized by three balanced and symmetrical signals. When an open fault occurs, one of the phases becomes disconnected, causing the voltage and current to drop. In Figure 2.2 (c) and Figure 2.2 (d) an open fault is induced at time, t = 16.67 ms. N. Bianchi *et al.* note that open circuit fault symptoms include torque pulsations due to unbalanced operation [BBZZ03]. In the next sections, the impact of these faults will be investigated, as to how they can lead to additional faults of the magnets and/or bearings.

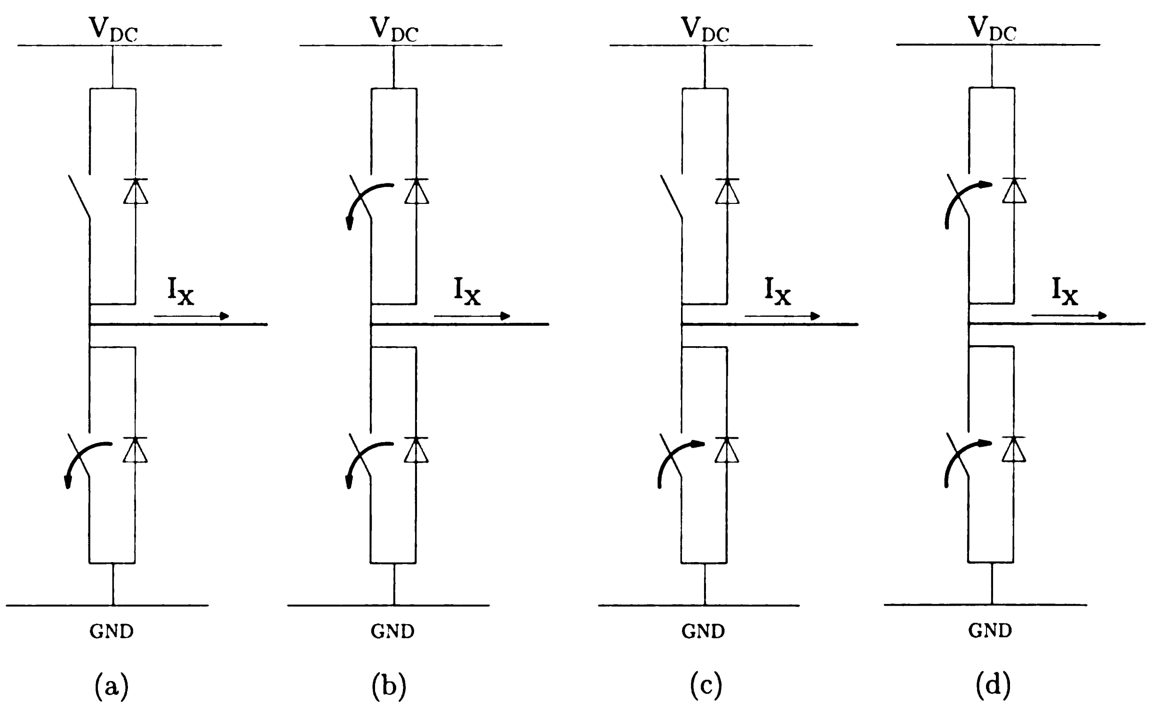

Figure 2.1. Inverter faults: (a) single switch open-circuit, (b) single phase open-circuit, (c) single switch short-circuit, and (d) single phase short-circuit.

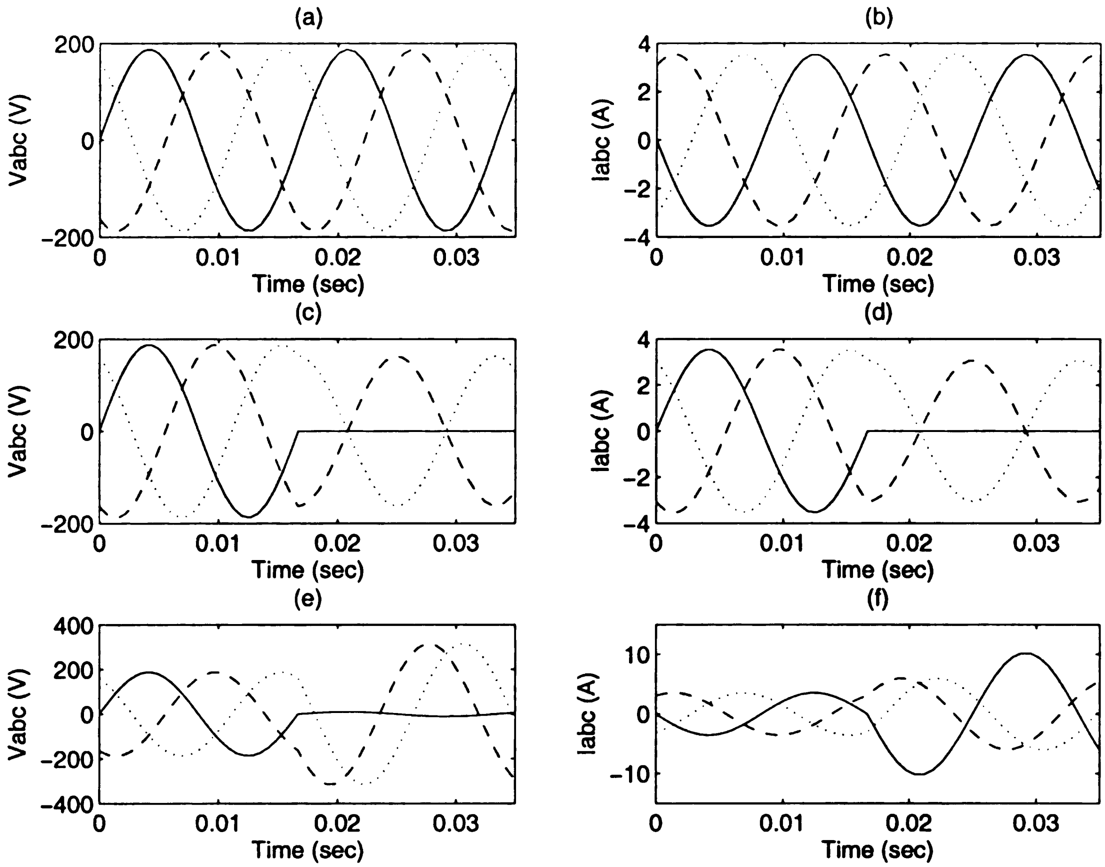

Figure 2.2. Three Phase Voltage and Current: (a) Normal Voltage, (b) Normal Current, (c) Open Fault Voltage, (d) Open Fault Current, (e) Short Fault Voltage, (f) Short Fault Current. Faults occur at t = 16.67 ms.

2.1.2 Short Circuit Faults

A short circuit fault can occur in a winding phase, between winding phases, or between two switches in the same phase. A fault that occurs in a single switch, as in Figure 2.1 (c), causes a high or low side of a phase to always be turned on, and thus results in large currents. Both switches in a phase can short, as in Figure 2.1 (d), and cause shoot–through to occur. This leads to severe damage to the power electronics and motor windings. The windings inside the motor can short phase–to–phase or short to the motor housing resulting in large currents. The waveforms in Figure 2.2 (e) and Figure 2.2 (f) are typical waveforms of voltage and current during a short fault. At time t = 16.67 ms, a short circuit fault occurs, the phase voltage drops and the phase current rises. Short circuit fault symptoms are similar to symptoms of an open fault, in that unbalanced operation occurs and produces torque ripples. Short circuit faults are more dangerous due to the large currents that they are capable of producing.

2.2 Secondary Faults

2.2.1 Permanent Magnets

Permanent magnet motors contain a rotor that is surrounded by magnets. The permanent magnets are either on the surface of the rotor or embedded in the rotor, as in Figure 2.3. The result is a constant rotor flux. However, there are exceptions, in particular, the flux of a permanent magnet can vary with temperature. To fully understand the effects of temperature, it is necessary to understand magnets and how they function in a motor.

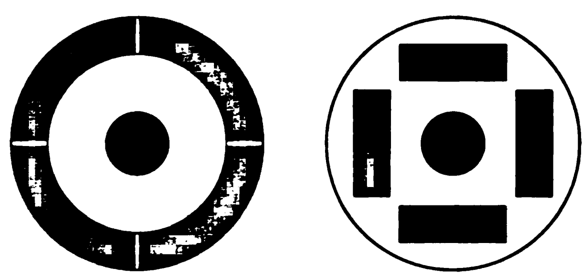

Figure 2.3. Permanent Magnet Rotors

Hysteresis Loop

The two key attributes of the state of a magnetic material are its magnetizing force (H) and its magnetic flux density (B). A graph relating these two properties, a hysteresis

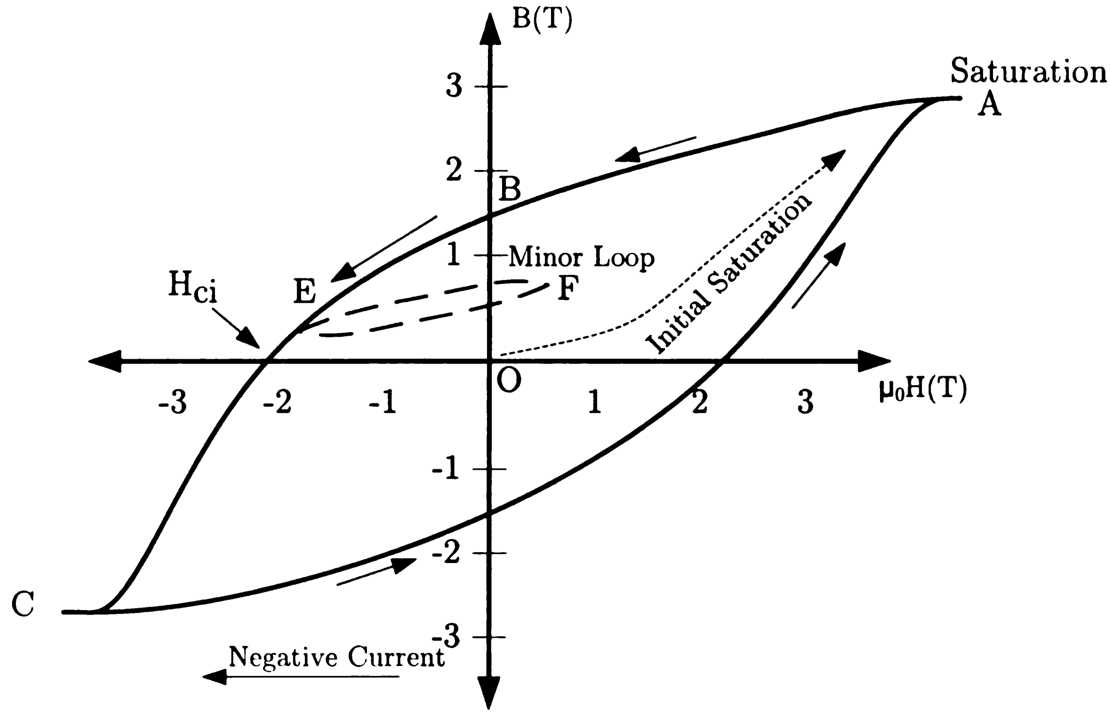

Figure 2.4. Hysteresis Loop

loop, is seen in Figure 2.4. In an un-magnetized sample, B = 0 and H = 0. The loop starts out at the origin and, when an external field is applied, B and H follow the loop going from the origin (O) to the saturation point (A).

In the application of a motor, the permanent magnet is operated in the second quadrant. When current is applied to the motor windings, the field created opposes the magnetic field of the permanent magnet. In Figure 2.4, when an increasing negative current, represented by the x-axis, is applied at point B, the operating point will slide down the main loop until the applied current is taken away at point E. The operating point will return to point F instead of the previous point on the main loop. When the negative current is re-applied at point F, the operating point will return to point E. This path is known as a minor hysteresis loop and is were the motor operates. In this area, the magnet can return to its original flux density if the magnetization remains constant. Demagnetization can occur if the magnetizing force reaches the coercive force required, known as H_{ci}. Quantifying the life of the magnet will be discussed in Chapter 4 Section 4.5.

2.2.2 Shaft Bearings

Bearing Currents

Bearings in motors are considered mechanical devices. However, they do possess electrical properties that affect their life time. Bearings are subject to currents that can cause significant damage if neglected. There are two classes of currents that can increase wear on the bearings. The first class is low frequency and the second class is high frequency.

Low Frequency Bearing Currents

According to D. McDonald *et al.*, low frequency bearing currents have been known since the 1920s [MG98]. They result from the interaction of DC or low frequency AC (50/60Hz) sources with asymmetries in the windings from manufacturing imperfections. These low frequency currents have been described by induced circulating currents that require a detailed and descriptive model of the motor winding in work published by S. Chen *et al.* [CL98]. Figure 2.5 illustrates a single winding with parasitic capacitances between phase windings and stator. The current entering the winding (I+ΔI) is different from the current leaving the winding (I-ΔI). The current, I, is composed of the fundamental harmonic and the additional current in the parasitic capacitance. This additional 2ΔI is known as the coupling current. The net current in the winding flows axially in the stator winding. This current induces a net magnetic flux linkage surrounding the motor shaft. This flux linkage links the stator case, shaft, and bearings, creating a circular pattern. The path of this circulating current can be seen in Figure 2.6. Bearing currents will flow when the shaft voltage

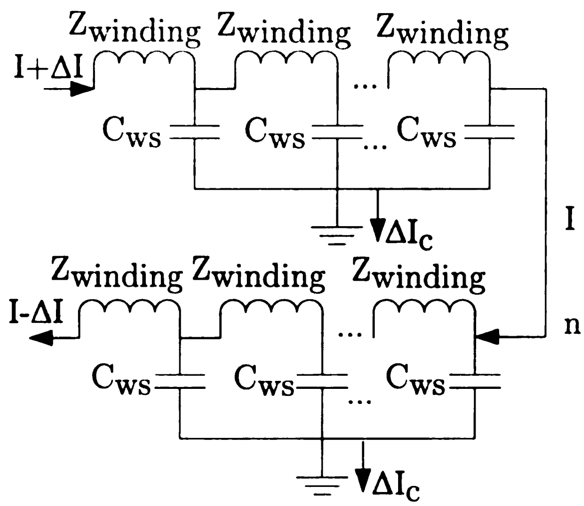

Figure 2.5. Single Winding Parasitic Capacitance Diagram and Coupling Currents

reaches a threshold that causes an electrical breakdown of the grease that is acting as an insulator. A. Muetze has published experimental results showing that the shaft voltage threshold is approximately 300 - 500 mV [Mue04]. A solution to this type of bearing currents is to use insulated bearings, which will break the circuit path preventing the flow of the current. These currents are not as damaging as high frequency bearing currents.

High Frequency Bearing Currents

High frequency bearing currents occur when an inverter-fed controller is used as a result of the high $\frac{dv}{dt}$. This class can be subdivided into two categories with two types in each [Mue04]. The first category is related to the common mode voltage, v_{common}, and its influence on the bearing voltage, $v_{bearing}$. The second category includes currents related to ground currents caused by the interaction between the common mode voltage and the parasitic capacitances in the motor.

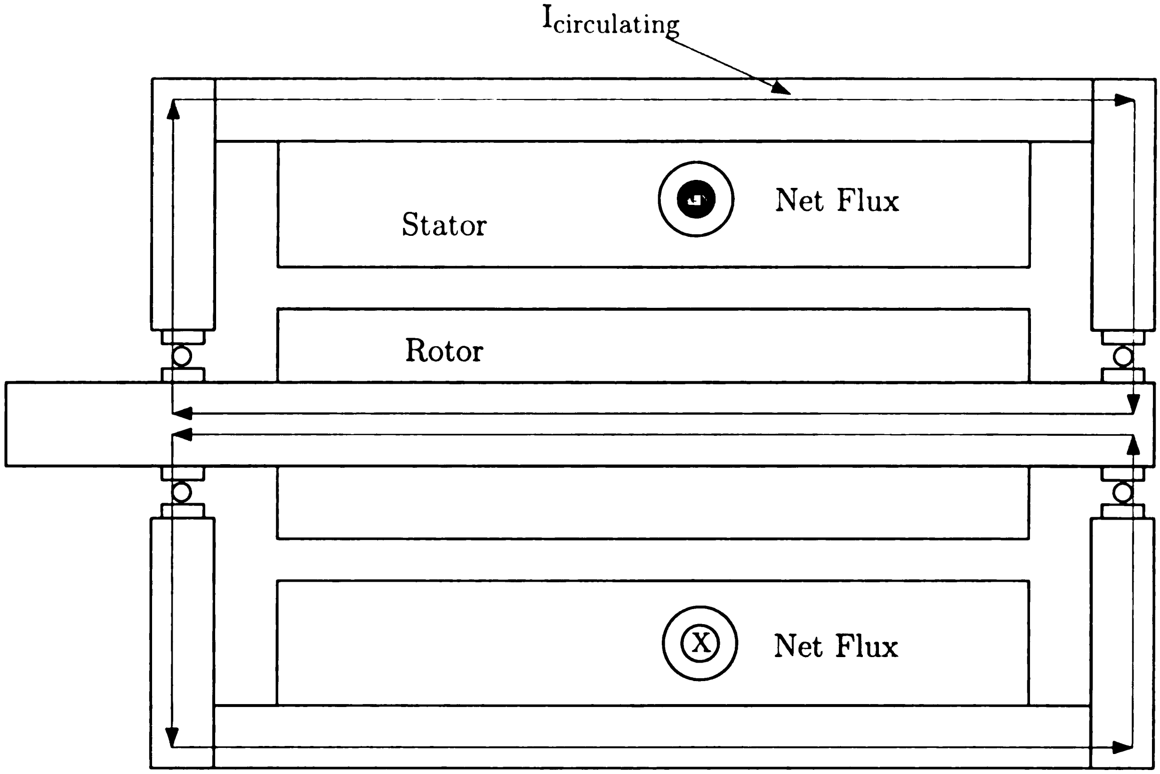

Figure 2.6. Motor Diagram of Low Frequency Circulating Bearing Currents

Common Mode Voltage

In motors driven with pure sinusoidal voltages, the three phase sources result in zero voltage at the motor's neutral point. However, this is not the case when inverter-fed PWM controllers are used. The common mode voltage (Figure 2.7) results from the PWM voltages not summing to zero. For non-sinusoidal sources, the common mode voltage can be determined according to Equation 2.1

$$v_{common} = \frac{v_{ag} + v_{bg} + v_{cg}}{3} \tag{2.1}$$

To determine the effects of a PWM inverter on the common mode voltage, two simulations were conducted. In the first simulation, a sinusoidal 230 V_{rms} three phase source is connected to a three phase load. The common mode voltage is determined by

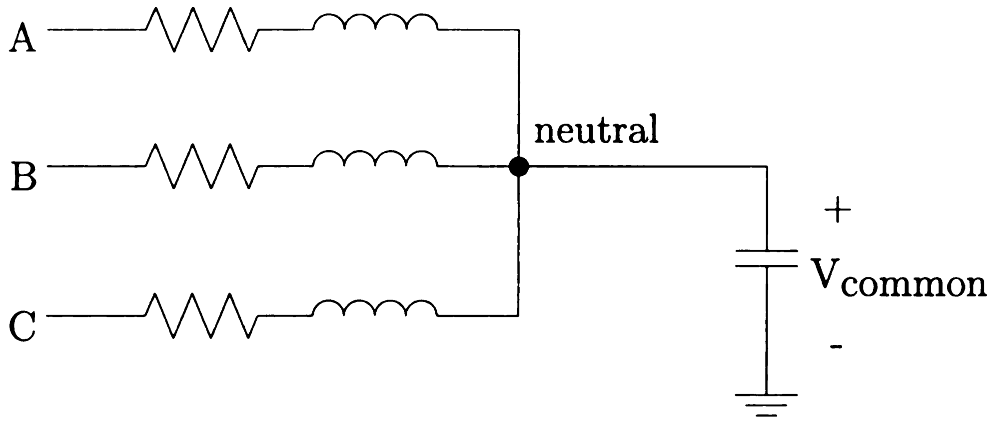

Figure 2.7. Common Mode Voltage

measuring the voltage at the neutral point of the load referenced to ground, similar to a motor with the neutral point available. In Figure 2.8, part (a) is a graph of the three phase sinusoidal source and part (b) is the common mode voltage. As expected, the three sinusoidal sources have a RMS value of 230 V_{rms}. The common mode voltage, which is defined by Equation 2.1, has a zero value.

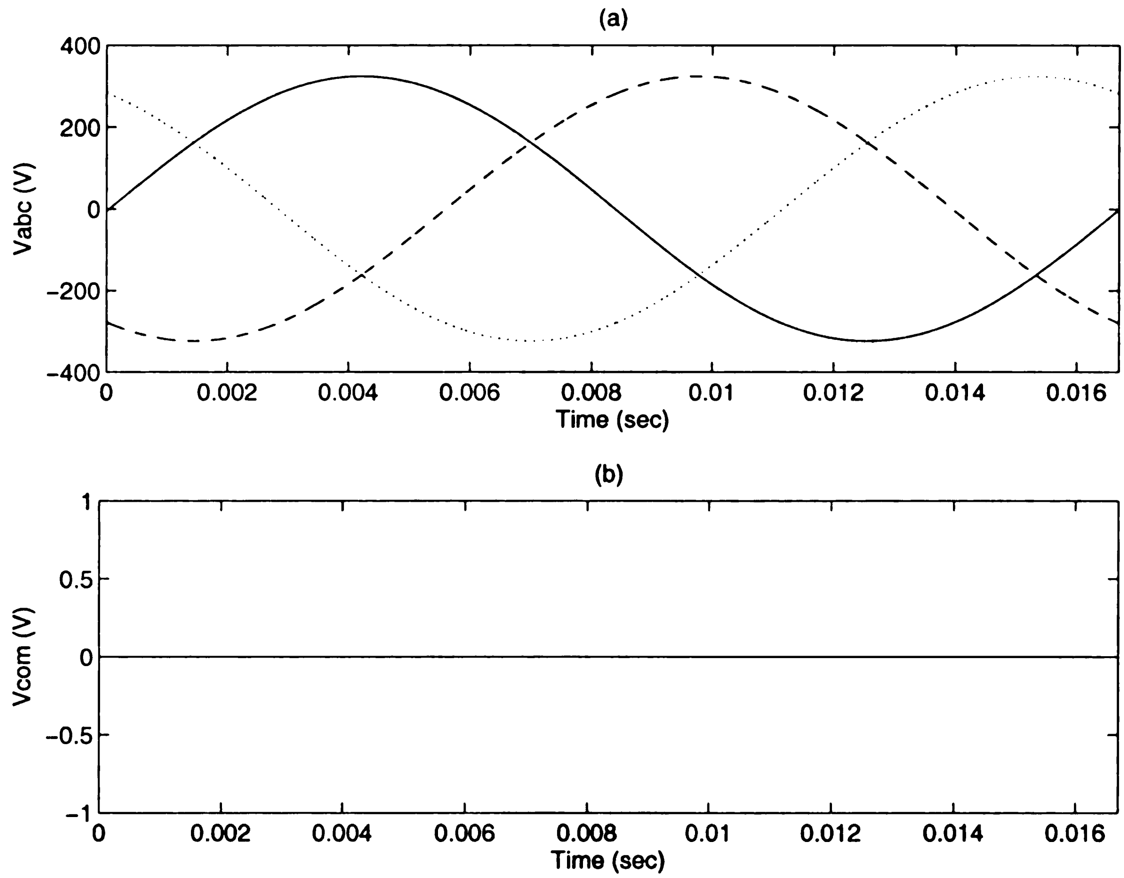

Figure 2.8. Sinusoidal and Common Mode Voltages Simulation Results: (a) 230V Three Phase Source, (b) Common Mode Voltage

In the second simulation, a PWM inverter is used in place of a sinusoidal source, it produces different results. In this simulation, a MOSFET inverter, operating at 2.5 KHz, is used to generate 230 V_{rms} with an identical three phase load from the previous simulation. The load voltage of the three phases is 230 V_{rms}, but the common mode voltage measured is 82.5 V_{rms}. The waveforms of this simulation are in Figure 2.9. In Figure 2.9, part (a) is a graph of the three phase PWM source and part (b) is the common mode voltage. A summary of results from each simulation is available in Table 2.1.

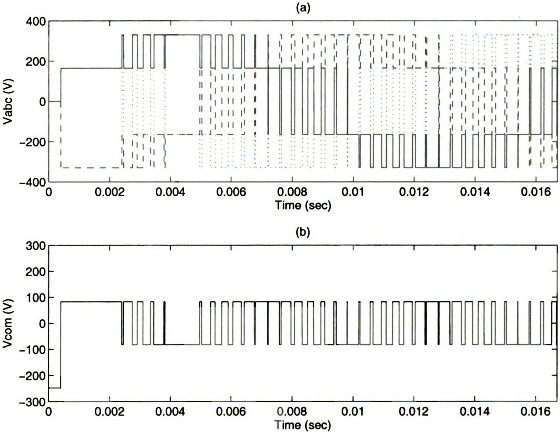

Figure 2.9. PWM and Common Mode Voltages Simulation Results: (a) 230V PWM Source, (b) Common Mode Voltage

	Sinusoidal	PWM
V_{rms}	229.9 V_{rms}	229.7 V_{rms}
V_{com}	0 V	82.5 V

Table 2.1. Common Mode Voltage Simulation Results

Capacitive Bearing Currents

The common mode voltage is directly related to the high frequency switching of the PWM inverter. The high frequency bearing currents are proportional to the common mode voltage and high frequency parasitic capacitances. The voltage across the bearings is due to the voltage divider of parasitic capacitances inside the motor (as shown in Figure 2.10), and this relationship is described by Equation 2.2. The four capacitances are C_{wf}, between the winding and frame, C_b, across the bearing, and C_{rf}, between the rotor and frame.

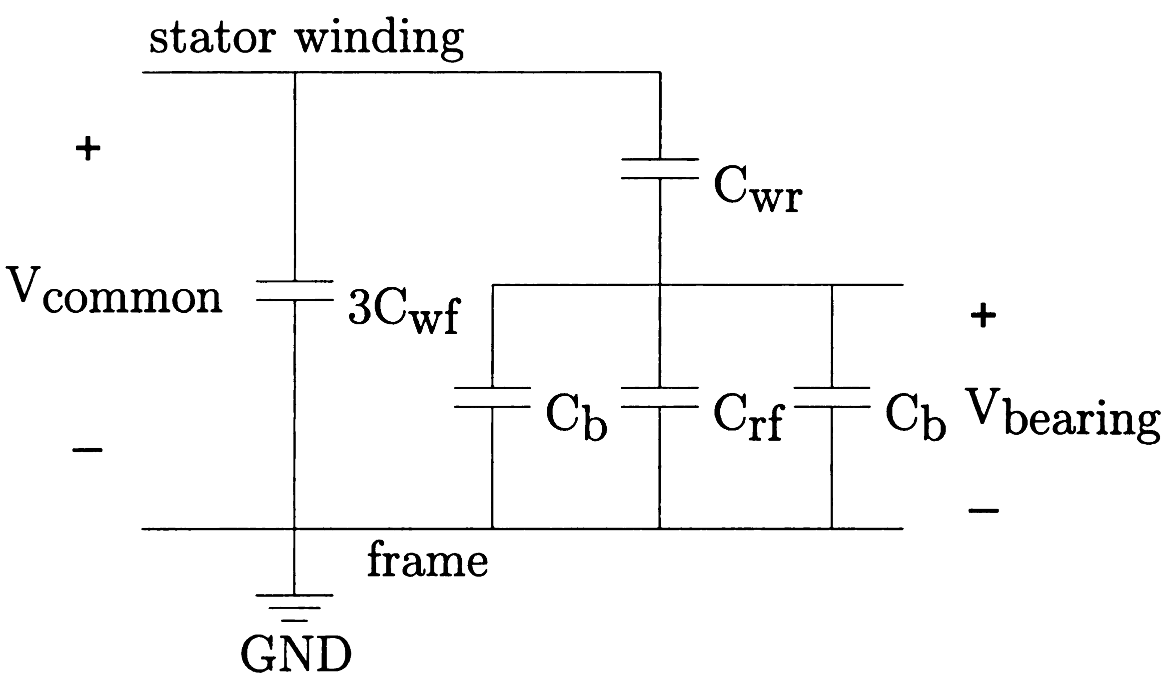

Figure 2.10. Bearing Voltage Due to Internal Motor Parasitic Capacitances and Common Mode Voltage

$$v_{bearing} = \frac{C_{wr}}{C_{wr} + C_{rf} + 2C_b} v_{common} \tag{2.2}$$

At low temperatures and high speed, the lubricating material in the bearing acts as a dielectric to form a capacitor between the inner and outer bearing walls. This, combined with a high frequency $v_{bearing}$, results in a current, $i_{bearing}$, with a range of 5 - 10 mA [Mue04].

$$i_{bearing} = C_{bearing} * \frac{dv_{bearing}}{dt} \tag{2.3}$$

At high temperatures and slow speed, the lubricating material acts like a resistor and has no insulating properties. Small voltages can result in currents up to 200 mA [Mue04].

$$i_{bearing} = \frac{v_{bearing}}{R_{bearing}} \tag{2.4}$$

Since these currents are relatively small compared to the other types of currents, they can safely be ignored when dealing with mitigation of bearing currents.

Electrostatic Discharge Currents

The electrostatic discharge currents occur inside the bearing. A circuit model of the bearing is in Figure 2.11. The bearing capacitance is represented by C_b and the bearing resistance is represented by R_b. In Figure 2.11, the bearing current, $i_{bearing}$, is defined by Equation 2.5:

$$i_{bearing} = \frac{v_{bearing}}{R_{bearing}} * \exp(\frac{-t}{T}) \tag{2.5}$$

where, $\mathrm{T} = R_{bearing} * C_{bearing}$.

In this type of bearing current, the common mode voltage increases enough that the bearing voltage surpasses the breakdown voltage threshold of the insulating property of the bearing lubricant and current flows. At low frequencies, the typical bearing

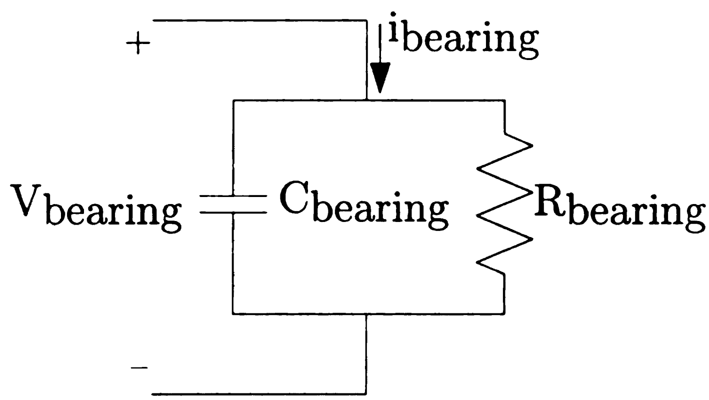

Figure 2.11. Electrostatic Discharge Current Model

voltage is 0.5 V and, at high frequency, the typical bearing voltage is 30 V [Mue04]. These voltages result in currents with magnitudes between 0.5 - 3 A [Mue04].

Circulating Bearing Currents

Similar to the low frequency currents, circulating ground currents encircle the motor shaft as seen in Figure 2.12. These currents result from the high frequency of the inverter and the parasitic capacitance between the stator winding and frame. The current i_{ground} (Equation 2.6) excites a magnetic flux (Equation 2.7) that produces the shaft voltage (Equation 2.8).

$$i_{ground} = \int H_{circ} dl \tag{2.6}$$

$$\Phi_{circ} = \mu \int H_{circ} dA \tag{2.7}$$

$$v_{shaft} = \frac{d\Phi_{circ}}{dt} \tag{2.8}$$

When the shaft voltage is large enough, it can break down the insulating properties of the bearing lubricant and results in a current flowing through the bearing. Bearing currents can vary between 0.5 - 20 A [Mue04].

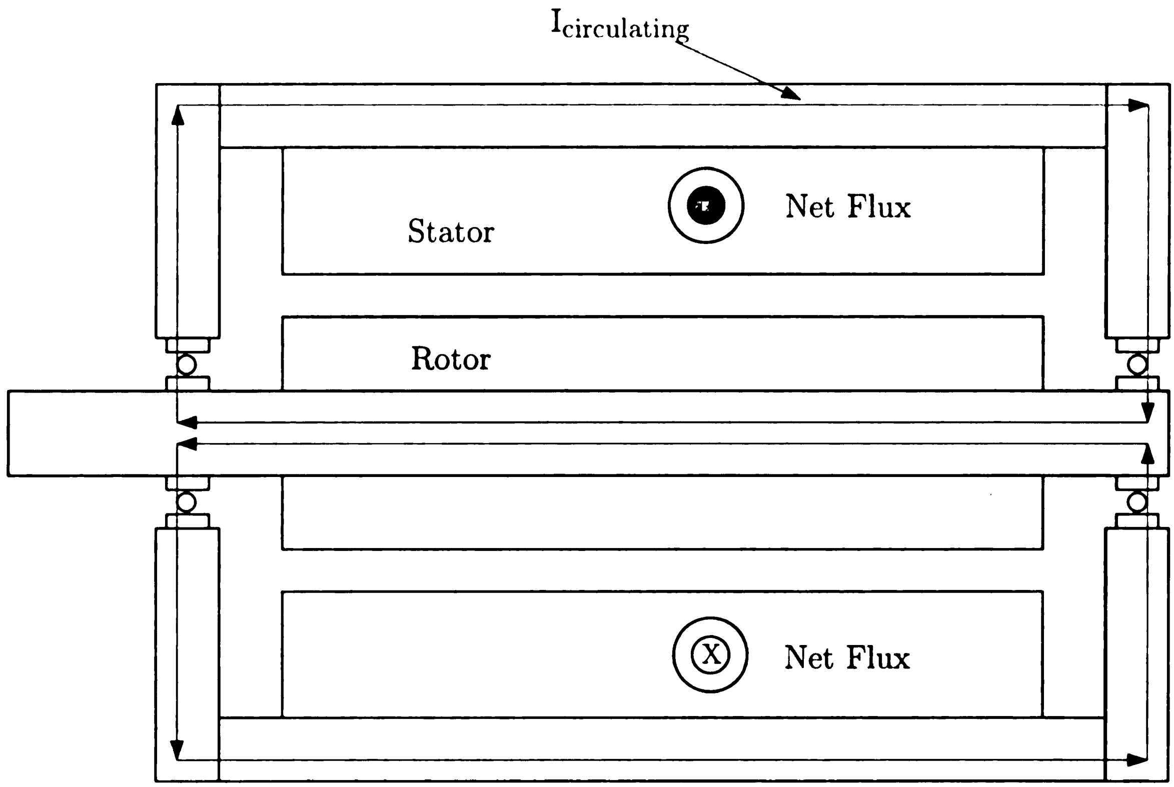

Figure 2.12. Circulating Bearing Currents

Rotor Ground Currents

These currents are proportional to the circulating bearing currents. Rotor ground currents result from the load end of the rotor being grounded. A current, $i_{rotor\ ground}$ (Equation 2.9), can flow through the motor shaft to the load, depending on the impedances of the rotor and stator as seen in Figure 2.13. The resulting current can damage bearings as it passes through them to the coupled load.

$$i_{rotor\ ground} = \frac{v_{shaft}}{z_{shaft}} \tag{2.9}$$

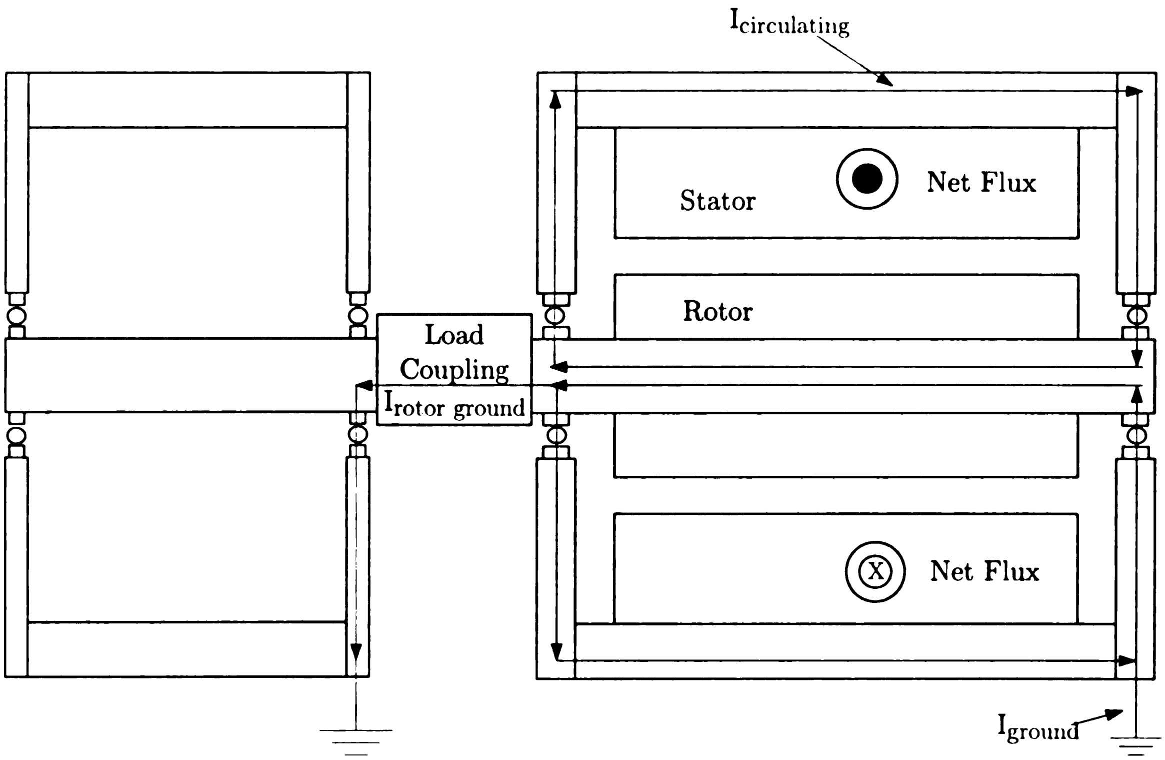

Figure 2.13. Rotor Ground Currents

Solutions to Bearing Currents

There are various solutions to reduce or mitigate bearing currents. These include but are not limited to:

- one or two insulated bearings
- hybrid or ceramic bearings
- filter on inverter to reduce/eliminate common mode voltage
- lower switching frequency
- insulated coupling between motor and load.

CHAPTER 3

Fault Mitigation and Fault Tolerant Design Solutions

There are three areas to consider when dealing with mitigation or prevention of faults. The areas are centered tapped DC-bus, hardware redundancy in the controller, and motor design.

3.1 Centered Tapped DC-bus

Adjusting the operation of the motor can reduce the effects of a fault and allow continued operating, but at a reduced level. A. Krautstrunk, shows that, in general, it is possible to run a three phase motor on only two phases [Kra99]. Figure 3.1 details the structure of a three phase inverter operated using only two phases.

If one phase opens, then it is possible to run the motor on the two remaining phases. By changing the current magnitude and phase in the healthy phases, a similar torque can be produced. Increasing the magnitude to $\sqrt{3}$ rated and shifting the phase to $\pi/3$, reduces the impact on stator current space vector (*i.e.* α-β coordinates) with respect to the previous. The result is torque that is very similar to the previous. It is necessary to shift the current phase by $\pi/3$ so that the torque ripple is reduced. To understand the reason for the larger currents, the following α-β-0 to

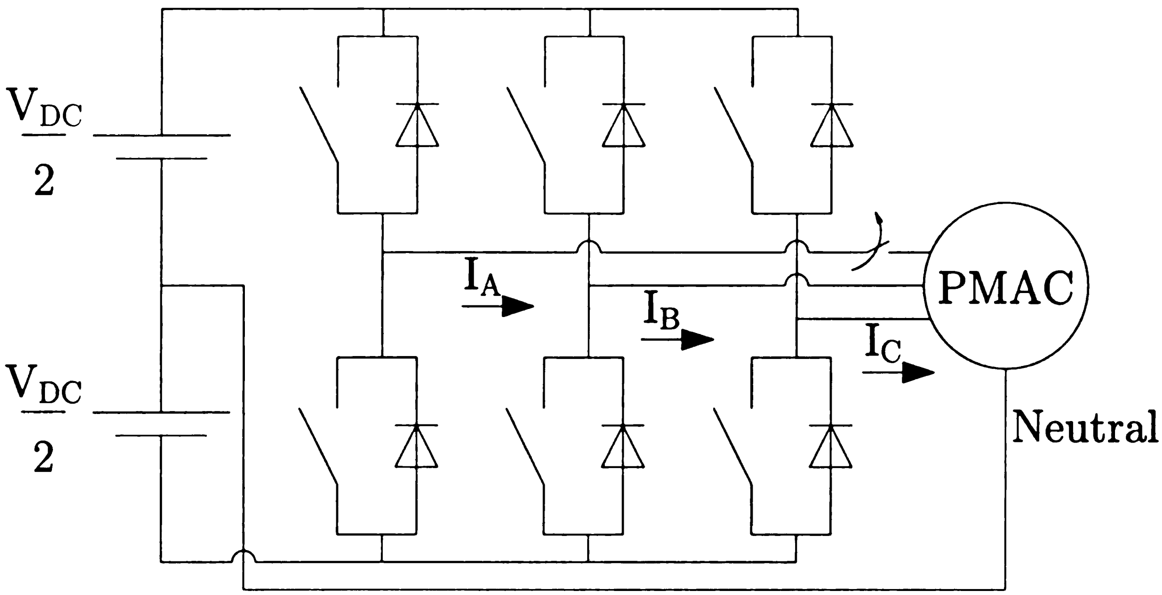

Figure 3.1. Center Tapped DC-bus Inverter Topology

a-b-c transformation is used.

$$\begin{bmatrix} i_a \\ i_b \\ i_c \end{bmatrix} = \begin{bmatrix} 1 & 0 & 1 \\ -\frac{1}{2} & \frac{\sqrt{3}}{2} & 1 \\ -\frac{1}{2} & -\frac{\sqrt{3}}{2} & 1 \end{bmatrix} \begin{bmatrix} i_\alpha \\ i_\beta \\ i_0 \end{bmatrix} \tag{3.1}$$

From Equation 3.1, the phase currents can be written as Equations 3.12, 3.13, and 3.14.

$$i_a = i_\alpha + i_0 \tag{3.2}$$

$$i_b = -\frac{1}{2} i_\alpha + \frac{\sqrt{3}}{2} i_\beta + i_0 \tag{3.3}$$

$$i_c = -\frac{1}{2} i_\alpha - \frac{\sqrt{3}}{2} i_\beta + i_0 \tag{3.4}$$

When the fault occurs, phase a opens and the current becomes zero. With $i_a = 0$, the equation for the current in phase a (Equation 3.2) is re-written as Equation 3.5.

$$0 = i_\alpha + i_0 \tag{3.5}$$

This can be re-written so that i_0 is in terms of i_α since $i_a = 0$, which results in Equation 3.6.

$$i_0 = -i_\alpha \tag{3.6}$$

Substituting Equation 3.6 into Equation 3.3 and Equation 3.4 results in the following phase b (Equation 3.7) and phase c (Equation 3.8) currents:

$$i_b = -\frac{3}{2} i_\alpha + \frac{\sqrt{3}}{2} i_\beta, \tag{3.7}$$

$$i_c = -\frac{3}{2} i_\alpha - \frac{\sqrt{3}}{2} i_\beta. \tag{3.8}$$

Under normal operating conditions, the sum of the three phase currents should equal zero. However, since phase a is open and $i_a = 0$, the three currents no longer sum to zero. The sum of currents in phase b and c is given by Equation 3.9.

$$i_b + i_c = -\frac{3}{2} i_\alpha + \frac{\sqrt{3}}{2} i_\beta + -\frac{3}{2} i_\alpha - \frac{\sqrt{3}}{2} i_\beta = -3 i_\alpha \tag{3.9}$$

With the mid-point of the DC-bus connected to the neutral point, a return path is available for the current, i_n, given by Equation 3.10.

$$i_n = -(i_b + i_c) = -3 i_\alpha = 3 i_0 \tag{3.10}$$

Figure 3.2 shows simulation results of phase currents, transformation currents, and torque. In Figure 3.2 part (a), the healthy three phase stator currents are monitored. At time t = 33 ms, phase a is faulted and disconnected. In Figure 3.2 part (b), the

α, β and zero sequence currents in the stator frame of reference are monitored. After the fault occurs and is compensated for, it can be seen that the α-β currents are maintained at nominal values. By keeping the α-β currents at the same values as before the fault, the same torque can be produced. In Figure 3.2 part (c), the torque is monitored. After the fault occurs and is recovered from, there is a slight torque ripple, but the ripple decreases and the torque becomes smooth again.

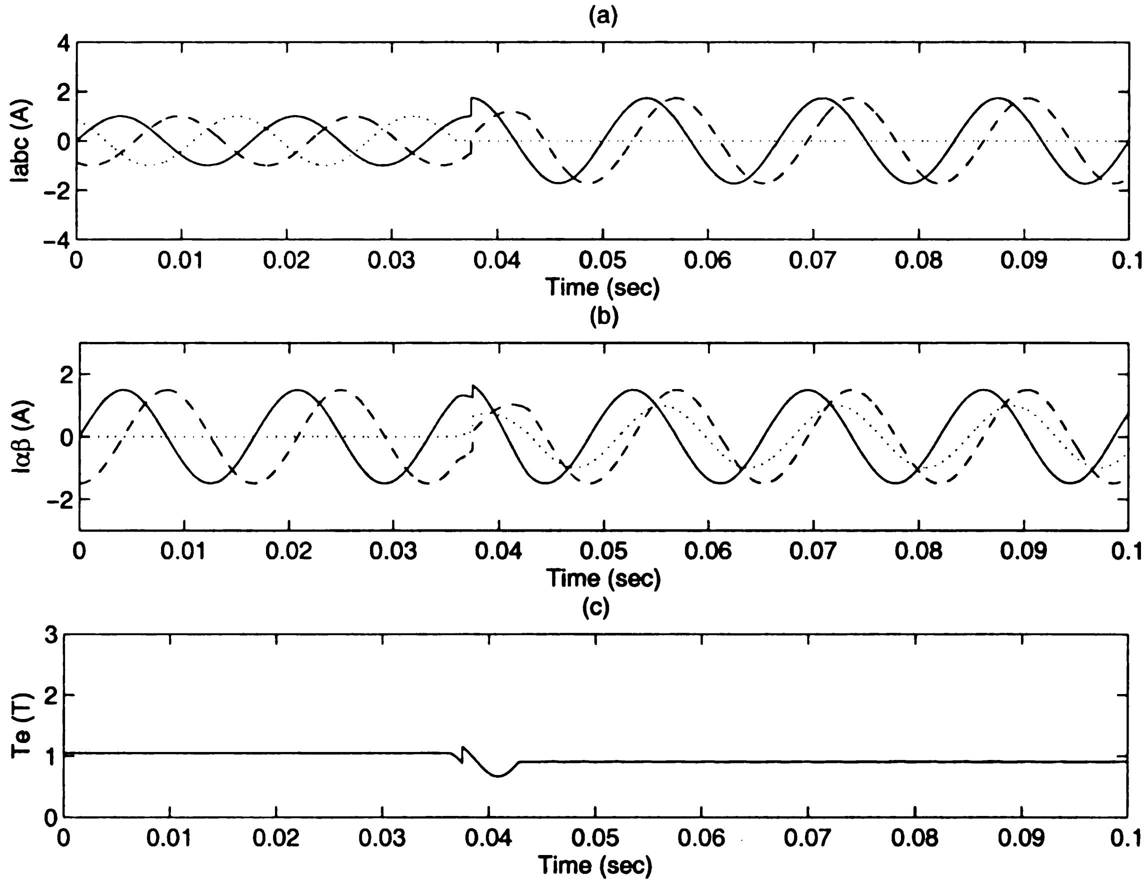

Figure 3.2. Center Tapped DC-bus Simulation Results

3.2 Hardware Redundancy in Controller

B.A. Welchco *et al.* have reviewed methods to design the controller of a motor with built-in redundancy. Using redundant power electronics, when a switch in the inverter fails, the controller can still function, maintaining near rated performance [WLJS03]. Figure 3.3 details the structure of a four phase inverter. By adding an additional

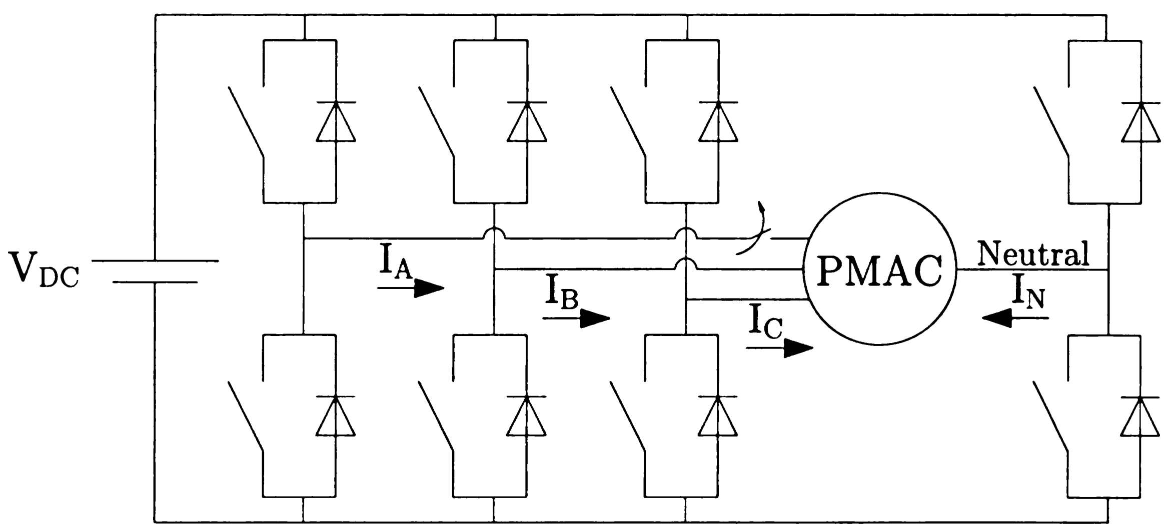

Figure 3.3. Redundant Phase Leg Inverter Topology

phase leg to the controller, it is possible to operate at rated power after a fault. The additional phase connects to the neutral of the motor. If any one phase fails, the neutral can be used to provide a return path [BBZZ03]. For this, it is required that the neutral point of the motor be accessible. In order to maintain rated torque, the healthy phase currents must increase to $\sqrt{3}$ times the rated healthy phase current and the 4th phase's current increases to 3 times the rated healthy phase current. This increase in currents requires over-sizing the inverter. To understand the reason for the larger currents, the following α-β-0 to a-b-c transformation is used.

$$\begin{bmatrix} i_a \\ i_b \\ i_c \end{bmatrix} = \begin{bmatrix} 1 & 0 & 1 \\ -\frac{1}{2} & \frac{\sqrt{3}}{2} & 1 \\ -\frac{1}{2} & -\frac{\sqrt{3}}{2} & 1 \end{bmatrix} \begin{bmatrix} i_\alpha \\ i_\beta \\ i_0 \end{bmatrix} \tag{3.11}$$

From Equation 3.11, the phase currents can be written as Equations 3.12, 3.13, and 3.14.

$$i_a = i_\alpha + i_0 \tag{3.12}$$

$$i_b = -\frac{1}{2}i_\alpha + \frac{\sqrt{3}}{2}i_\beta + i_0 \tag{3.13}$$

$$i_c = -\frac{1}{2}i_\alpha - \frac{\sqrt{3}}{2}i_\beta + i_0 \tag{3.14}$$

When the fault occurs, phase a opens and the current becomes zero. With $i_a = 0$, the equation for the current in phase a (Equation 3.12) is re-written as Equation 3.15.

$$0 = i_\alpha + i_0 \tag{3.15}$$

This can be re-written so that i_0 is in terms of i_α since $i_a = 0$, which results in Equation 3.16.

$$i_0 = -i_\alpha \tag{3.16}$$

Substituting Equation 3.16 into Equation 3.13 and Equation 3.14 results in the following phase b (Equation 3.17) and phase c (Equation 3.18) currents:

$$i_b = -\frac{3}{2}i_\alpha + \frac{\sqrt{3}}{2}i_\beta, \tag{3.17}$$

$$i_c = -\frac{3}{2}i_\alpha - \frac{\sqrt{3}}{2}i_\beta. \tag{3.18}$$

Under normal operating conditions, the sum of the three phase currents should equal zero. However, since phase a is open and $i_a = 0$, the three currents no longer sum to zero. The sum of currents in phase b and c is given by Equation 3.19.

$$i_b + i_c = -\frac{3}{2}i_\alpha + \frac{\sqrt{3}}{2}i_\beta + -\frac{3}{2}i_\alpha - \frac{\sqrt{3}}{2}i_\beta = -3i_\alpha \tag{3.19}$$

With the additional inverter leg connected to the neutral point, a resulting current, i_n, will exist to balance out the sum of i_b and i_c and is given by Equation 3.20

$$i_n = -(i_b + i_c) = -3i_\alpha = 3i_0. \tag{3.20}$$

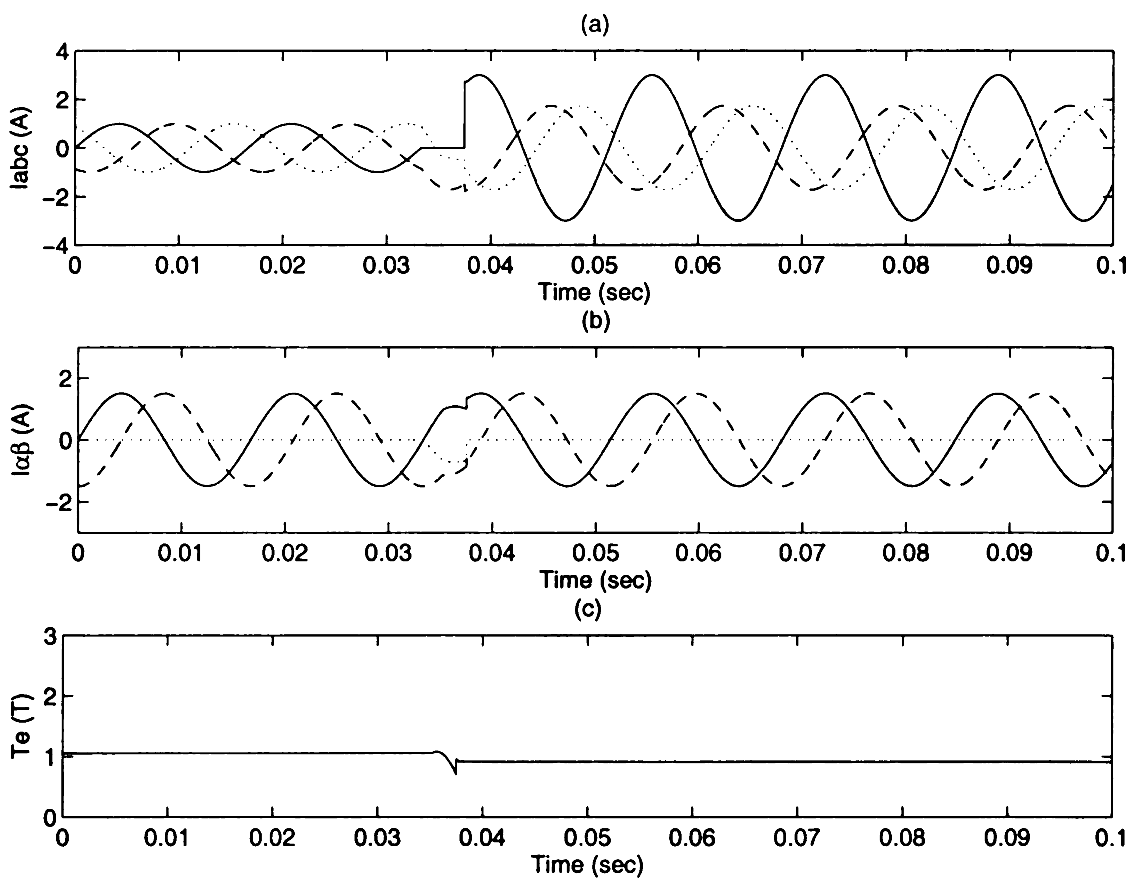

Figure 3.4. Redundant Phase Leg Inverter Simulation Results

Simulation results indicate that this technique provides performance very similar to normal operation. Figure 3.4 shows current and torque before and after a fault. In Figure 3.4 part (a), the healthy three phase currents are monitored. At time t = 33 ms, phase a is faulted and the controller isolates phase a, disconnecting it from the motor. In Figure 3.4 part (b), the α, β and zero sequence currents in the stator frame of reference are monitored. After the fault occurs and is mitigated, it can be seen that the α-β currents are maintained near nominal values. By keeping the α-β currents near the same values as before the fault, the same torque will be produced. The controller adjusts the currents in the remaining healthy phases b and c by increasing amplitudes and adjusting the phase angle as in Equations 3.17 and 3.18. By adjusting the phase angle from $\frac{2\pi}{3}$ to $\frac{\pi}{3}$, the torque ripple is reduced. To make up for phase a, the switch connected to the neutral point provides a return path for the current, defined by Equation 3.20, to balance the new currents from phases b and c. In Figure 3.4 part (c), the torque is monitored. After the fault occurs and is recovered from, there is a slight ripple, but the ripple decreases and the torque becomes smooth again.

3.3 Motor Design

Instead of designing a motor and controller that react to a fault, the idea of a fault tolerant motor is that it will operate at rated conditions even under a fault. The most common motor and controller faults are open windings, shorted windings, open switches, and shorted switches. Behavior under, these faults are the criteria to determining if a machine is fault tolerant.

3.3.1 Reducing Short Circuit Currents

The greatest threat to the health of a motor is currents above rating. Works published by P.H. Mellor *et al.*, B.C. Mecrow *et al.*, and A.G. Jack *et al.* support designing a motor that is able to limit short-circuit currents to rated values. This results in a motor that is able to withstand short circuit faults that would normally be catastrophic [MAOR03, MJHC96, JMH96]. One way to limit high currents is to design a motor with a 1 per-unit inductance [MAOR03]. Then, even if there is a short, the inductance of the windings will limit the current to its rated value. During a short circuit at the terminals of the motor, the peak current can be determined by Equation 3.21 [MJHC96].

$$I_{pu} = \frac{\Psi_{flux}}{R_{pu}/j\omega_{pu} + L_{pu}} \tag{3.21}$$

Typically, the per-unit resistance is relatively small that it can be ignored, so that Equation 3.21 can be rewritten as Equation 3.22

$$I_{pu} = \frac{\Psi_{flux}}{L_{pu}} \tag{3.22}$$

In Equation 3.22, the current will be one per-unit as long as Ψ_{flux} equals L_{pu}.

3.3.2 Multiple Phases Topologies

If a fault occurs, and it is required that rated power or torque be maintained, then using multiple phases will allow for less over-rating of phases [MJHC96]. For example, it is possible to run a three phase motor on two phases; however, to maintain the same power output as prior to the fault, phase currents must be increased. To determine how much of an increase in ratings is required, Equation 3.23 can be used. F is the fault tolerant factor, and n is the number of phases. The fault tolerant factor is the factor by which the power electronics and motor should be over-rated [JMH96].

$$F = \frac{n}{n-1} \tag{3.23}$$

The over-rating has been calculated for several different values of n in Table 3.1.

n - number of phases	F - fault tolerant rating factor
3	1.50
4	1.33
6	1.20

Table 3.1. Fault Tolerant Rating Factor

The more phases there are, the less over-rating is required per phase. For example, let's take a three phase motor with rated current of 1 pu that produces a torque of 3 pu as noted in Equation 3.24. If one of the phases has a fault and is disconnected by the controller, then there would be only two phases to produce the same torque. Using the data from Table 3.1, the fault tolerant rating factor for a three phase motor is 1.50. Therefore, if the faulted two phase motor is to produce the same torque as a three phase motor, then a higher current will be required in the remaining healthy phases. For this example with only two phases, the current is described by Equation 3.25. It should also be noted that the power electronics must also be rated above the fault tolerant rating factor to prevent over-rating failures.

$$I = 1pu * 3(n) \rightarrow T = 3pu \tag{3.24}$$

$$I = 1pu * 2(n) * 1.5(F) \rightarrow T = 3pu \tag{3.25}$$

3.3.3 Isolated Windings

If a short-circuit fault occurs in one phase, it is possible to reduce its effects on its neighboring phases. Three problems can occur depending on the layout of the windings: there can be magnetic interference, thermal interference, and phase to phase faults. It is possible that by isolating each phase to its own slot(s), the above three cases can be reduced or eliminated [MJHC96]. Figure 3.5 shows an example of a

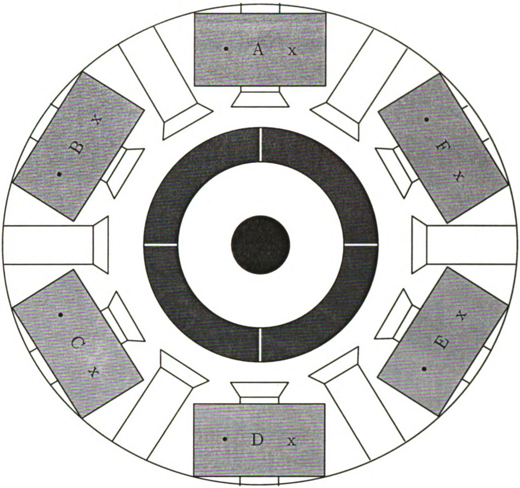

Figure 3.5. Isolated/Multiple Phase Winding Topology

six phase stator. Each phase is isolated to two adjacent slots and no two phases share a slot. So if a fault were to occur in a phase, it would be restricted to that phase and only that phase due to the separation of phases. This would significantly reduce and prevent phase to phase faults. Additionally, magnetic isolation and thermal isolation would increase as well. Magnetic isolation means that if a large fault occurs in one of the phase windings, due to the isolation of the phases, no large voltages would be induced into another phase. Along the same lines, thermal isolation increases because any phase fault is isolated to one or two slots and only the phase in that slot. By isolating the phase windings, each phase is modular, in a sense, and independent of the others.

CHAPTER 4

Reliability Models

The failure rate of a device can be described by the curve in Figure 4.1. According

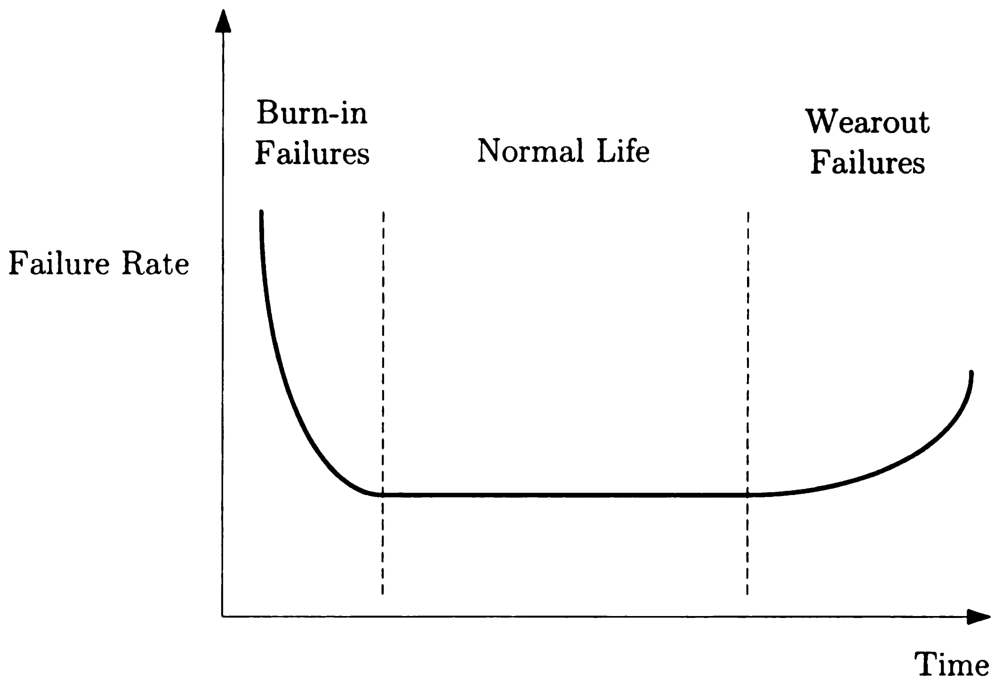

Figure 4.1. Failure Rate Curve

to National Semiconductor, this curve represents the failure rate over the lifetime of a component or system [Nat04]. There are two areas of high failure rate, early and wearout failures. Early failures are most often due to manufacturing defects of the device. Wearout failures are due to natural aging of the device. In the middle, lies the failure rate during the normal life time of the device, which is constant, and used to model the expected life time of systems. The reliability of a system can be determined from the failure rates of the components that make it up. It is important to note that the reliability of a system is related to the operating conditions and parameters, known as covariates. The covariates represent stress on the device, which can include, but are not limited to, current, voltage, and temperature as noted by P.V.N. Prasad *et al.* The failure rate of a system can be described by Equation 4.1 [PR02].

$$\lambda(t, z) = \lambda_0(t) exp(z\beta) \tag{4.1}$$

where,

- λ_0 – the base line failure rate
- z – a vector containing covariates
- β – a vector of regression coefficients

Under rated conditions, the reliability of a system is a constant function of time, $R_0(t)$, the base line reliability. The reliability of the system including the covariates is given by Equation 4.2 [PR02].

$$R(t, z) = R_0(t) exp(-z\beta) \tag{4.2}$$

Under different operating parameters, there are de-rating factors associated with the current, voltage, and temperature that are outside of the normal operating parameters. These de-rating factors negatively affect the reliability. As a result, the system reliability can be modeled as a constant base reliability plus an additional factor for each rating above the normal. An example of such rating would be operating a device at a higher temperature that it is rated for, or at a higher power level. According to Reliasoft, this is common practice for accelerated life testing [Rel04b]. By applying an increased stress over a short time interval, we can simulate a lesser stress over a longer time period.

4.1 Types of Models

4.1.1 Arrhenius Life Model

A common model for accelerated life testing is the Arrhenius life-stress model [Rel04a]. This model uses temperature as a stress variable. The model is derived from the Arrhenius reaction rate equation given by Equation 4.3 [Rel04a].

$$R(T) = A * exp(\frac{-E_A}{KT}) \tag{4.3}$$

where,

- R – speed of reaction or failure rate
- T – absolute temperature (Kelvin)
- K – Boltzman's constant
- E_A – activation energy
- A – model parameter

The reaction represents the rate of decay and is useful for representing the life of a device when temperature is a stress. As the temperature increases, the energy available to initiate a reaction increases. The activation energy denoted by E_A is the amount of energy required for a molecule to take part in the reaction. As the temperature increases, the reaction increases, reducing the life of the component.

The Arrhenius life-stress model is derived from the reaction rate equation by assuming life time is proportional to the inverse reaction rate of the process. Equation

4.4 describes the life time [Rel04a].

$$L(V) = C * exp(\frac{B}{V}) \tag{4.4}$$

where,

- L – quantitative life measurement (hours)
- C – model parameter
- V – stress (based on temperature in Kelvin)
- B – $\frac{E_A}{K}$

As the reaction rate increases, due to the temperature increasing, graphing the model in Figure 4.2, shows an exponential decay of life time as the stress increases. The dashed line corresponds to a higher activation energy and the solid line corresponds to a lower activation energy.

4.1.2 Exponential Life Model

The exponential life model describes a stress as exponentially aging a material. When the stress is large enough, rate of decay will start to have a negative impact on the life.

$$L(E) = C * exp(-P) \tag{4.5}$$

where,

- L – quantitative life measurement (hours)
- P – stress
- C – model parameter

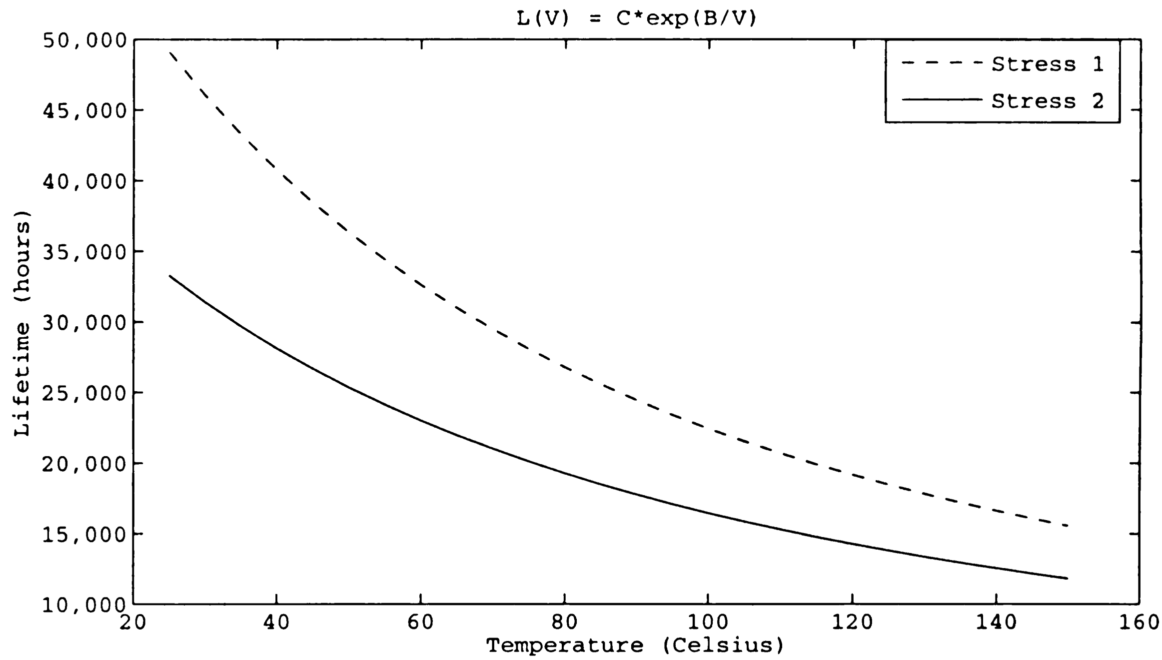

Figure 4.2. Arrhenius Life Model

In Figure 4.3, the life is graphed and shows an exponential decay of life time as the stress increases. The dotted line represents a lesser stress compared to the solid line which represents a greater stress. As the stress increases, the life decreases.

4.2 Modeling Device Reliability

System reliability can be calculated based on the summation of the individual components of a system. Understanding the reliability (or lifetime) of these components allows for determining the overall system reliability under fault recovery operation. Given a standard three phase PMAC motor, there are several areas that play a significant role in the life of the system. These areas are the power semiconductor switches (MOSFETs or IGBTs), magnet wire/winding insulation, permanent magnets, and shaft bearings.

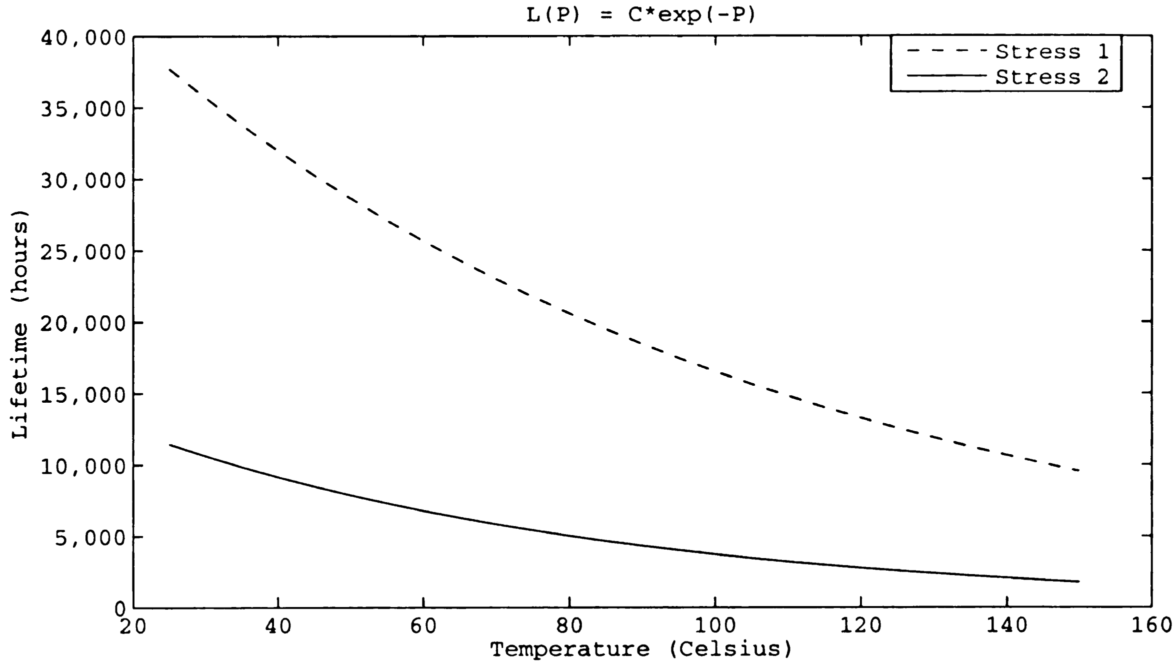

Figure 4.3. Exponential Life Model

4.3 Modeling Semiconductor Life

The lifetime of power semiconductors can be modeled as a function of the junction temperature and operating power level of the device, which corresponds to the average power dissipated. Measuring the junction temperature is difficult, so the ambient temperature can be used to calculate the junction temperature. The failure rate of the device can be modeled using the Arrhenius lifetime model. The stress will be the temperature.

The junction temperature can be calculated based on the power dissipated and the thermal resistance of the package from the junction to the ambient [Nat04]. Equation 4.6 provides this calculation [Nat04].

$$T_J = T_A + P_D \Theta_{JA} \tag{4.6}$$

where,

- T_J – junction temperature ($^{\circ}C$)
- T_A – ambient temperature ($^{\circ}C$)
- P_D – average power dissipated by device (W)
- Θ_{JA} – thermal resistance from junction to ambient ($^{\circ}C/$W)

The terms P_D and Θ_{JA} are defined by the manufacturer's specification and can be found on a device's datasheet. P_D can be calculated using Equation 4.7.

$$P_D = P_R + P_S \tag{4.7}$$

where,

- P_R – power dissipated when device is on (W)
- P_S – power dissipated while switching (W)

The life time can then be calculated using Equation 4.8.

$$L(T_J) = L_0 * exp(-B * \Delta T_J) \tag{4.8}$$

where,

- L – quantitative life measurement (hours)
- ΔT_J – stress defined by Equation 4.9
- L_0 – quantitative normal life measurement (hours)
- B – $\frac{E_A}{K}$

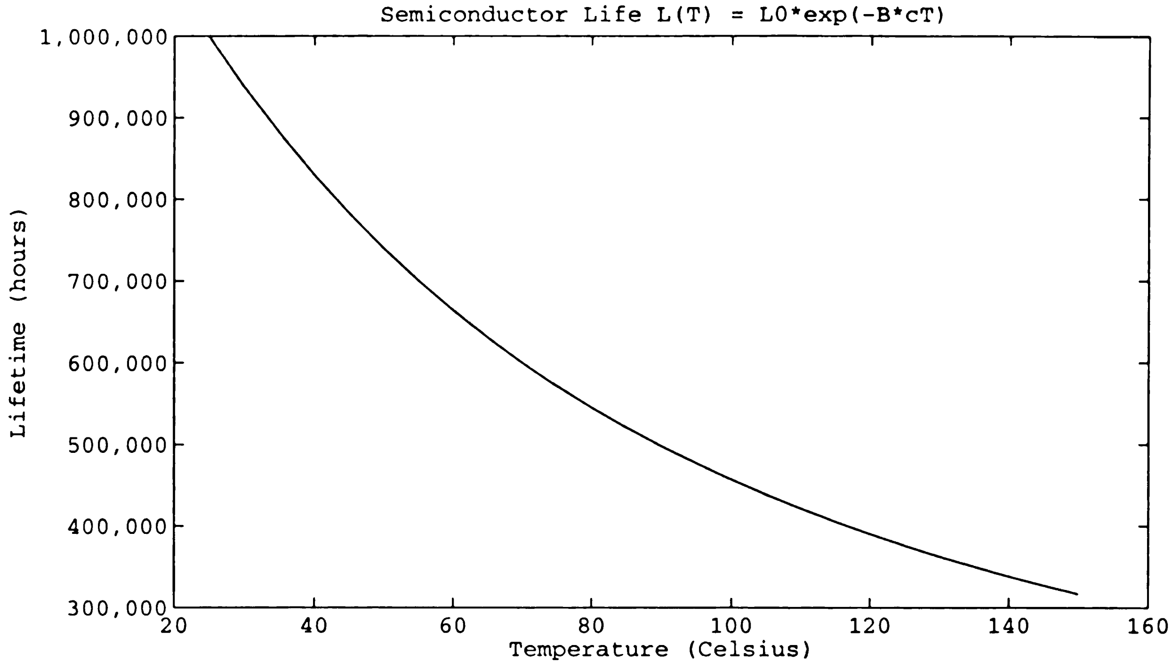

Figure 4.4. Semiconductor Life Model

$$\Delta T_J = \frac{1}{T_A} - \frac{1}{T_J} \tag{4.9}$$

where,

- T_A – the ambient temperature (Kelvin)
- T_J – junction temperature (Kelvin)

The failure rate is the inverse to the lifetime, $L_{semiconductor}$. The failure rate is described by Equation 4.10.

$$\lambda_{semiconductor} = \frac{1}{L_{semiconductor}}. \tag{4.10}$$

Figure 4.4 shows the lifetime predicted by the model in Equation 4.8.

4.4 Modeling Insulation Life

In work published by G.C. Montanari, the life time of winding insulation can be modeled based on the temperature of the material [Mon00]. This makes the Arrhenius life model a suitable formula for modeling the life of winding insulation. Winding insulation breaks down due to stress such as temperature and other factors. However, determining the temperature of the windings can prove to be difficult. It is possible to estimate the temperature based on current and power.

4.4.1 Estimating Winding Temperature

The winding temperature of the motor can be estimated from the power losses of the motor. There are two types of power losses: copper and iron losses. Copper losses occur due to the resistance of the windings and the current that passes through. Iron losses, also known as eddy losses, result from eddy currents that form in the core of the motor. In this model, we will neglect iron losses so as to simplify the analysis. At room temperature, the stator resistance and current entering a single phase can be measured. Multiplying by the number of phases, n, results in the total phase power losses. The power can be calculated using Equation 4.11.

$$P = n * |I|^2 * R \tag{4.11}$$

If the phase currents are increased, the winding losses will increase by the square. As the losses increase, the temperature of the windings increases. For example, if a healthy three phase motor is running at rated current of 1pu and has a resistance of 0.1pu, then the losses calculated are given by Equation 4.12.

$$P_{losses-1} = 3 * |1|^2 * 0.1 = 0.3pu \tag{4.12}$$

Given the same motor, operating on two phases, to produce the same torque, the currents will need to be increased by $\sqrt{3}$. In this case, the current will be $\sqrt{3}$pu and if we assume the resistance to be 0.1pu, then the losses can be calculated by Equation 4.13.

$$P_{losses-2} = 2 * |\sqrt{3}|^2 * 0.1 = 0.6pu \tag{4.13}$$

The increase in power is given by Equation 4.14.

$$P_{increase} = \frac{P_{losses-2}}{P_{losses-1}} = \frac{0.6pu}{0.3pu} = 2.0 \tag{4.14}$$

If the healthy three phase motor had a measured temperature of T_{room}, then using a centered tapped DC-bus and the above estimations, the new temperature rise, $T_{new-rise}$, would increase by approximately 2.0 times. An example has been provided in Figure 4.5. If the ambient temperature was 40 $°C$, and the hot-spot temperature rise due to the losses is 20 $°C$, then the temperature increases to 60 $°C$. If the currents are increased and the temperature rise is doubled to 40 $°C$, then the temperature increases to 80 $°C$. This approximation depends heavily on the cooling method of the motor and motor housing. Obviously, for active cooling methods, this approximation may not be accurate.

4.4.2 Insulation Life Model

The lifetime of insulation can be modeled using stress as an aging factor, according to G.C. Montanari *et al.*[MMS02]. The stress can be voltage, temperature, or mechanical vibration, etc. The life can be approximated by Equation 4.15, using temperature as a stress.

$$L_{insulation} = L_0 * exp(-B * \Delta T) \tag{4.15}$$

where,

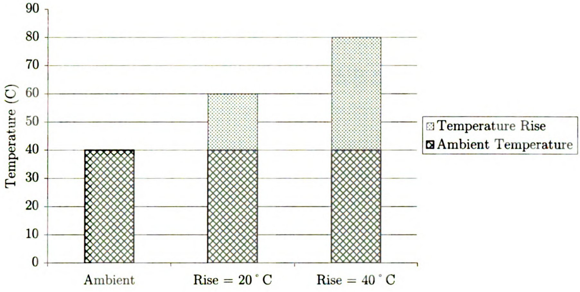

Figure 4.5. Temperature Rise

- $L_{insulation}$ – quantitative life measurement (hours)
- L_0 – quantitative normal life measurement (hours)
- B – $\frac{E_A}{K}$
- Δ T – thermal stress defined by Equation 7.11

$$\Delta T = \frac{1}{T_A} - \frac{1}{T} \tag{4.16}$$

where,

- T_A – the ambient temperature (Kelvin)
- T – component temperature (Kelvin)

The failure rate is inverse to the lifetime, L. The failure rate is described by Equation 4.17.

$$\lambda_{insulation} = \frac{1}{L_{insulation}}. \tag{4.17}$$

Figure 4.6 shows the lifetime predicted by the model in Equation 4.15.

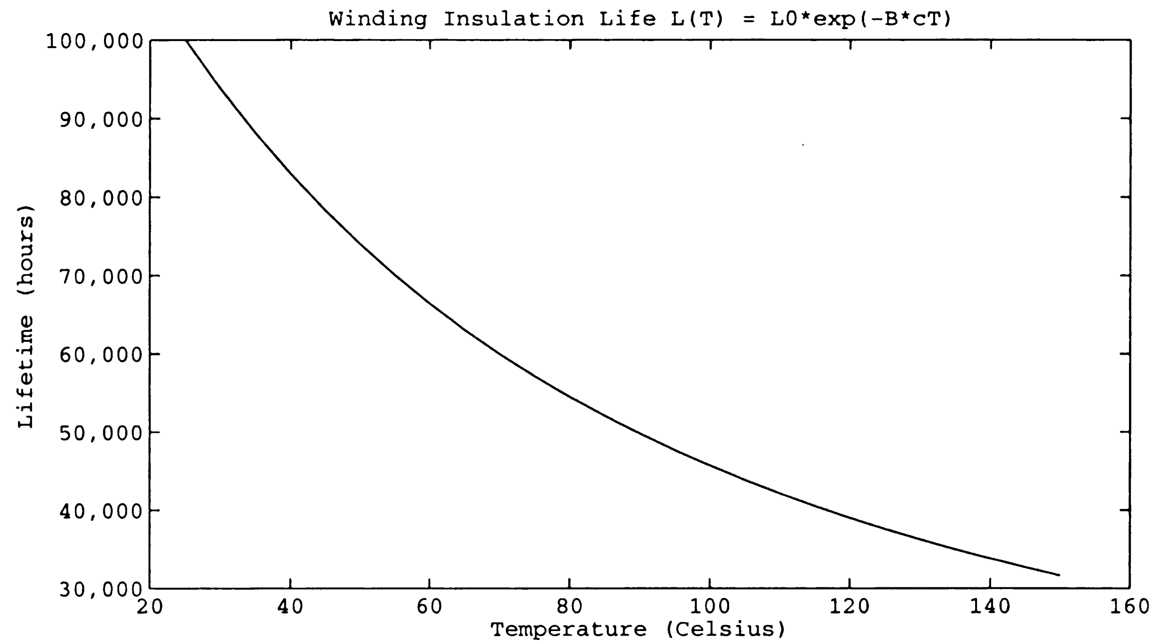

Figure 4.6. Winding Insulation Life

4.5 Modeling Lifetime of Permanent Magnets

4.5.1 Damage to Permanent Magnets

At high temperatures, it is possible to permanently damage a magnet so that it can no longer provide the flux necessary for operation. The material of the magnet determines the amount of change in the field as temperature changes.

Reversible loss of magnetization occur when temperatures increase and the hysteresis loop shrinks, moving the operating point. This results in less flux. The hysteresis loop and recoil line return to its original shape after the temperature returns to its normal value. For NdFeB magnets, T.J.E Miller notes, as the temperature increases, the remanence decreases by $0.11\%/°C$ and the intrinsic coercivity decreases by 0.60 $\%/°C$[Mil89].

Other loss of magnetization, known as, irreversible loss of magnetization is more dangerous due to the fact that it requires re-magnetizing the material. During operation, if the operating point falls to a lower curve, there can be a loss in the flux density. In Figure 4.7, the original operating point is along the path from point a to point A

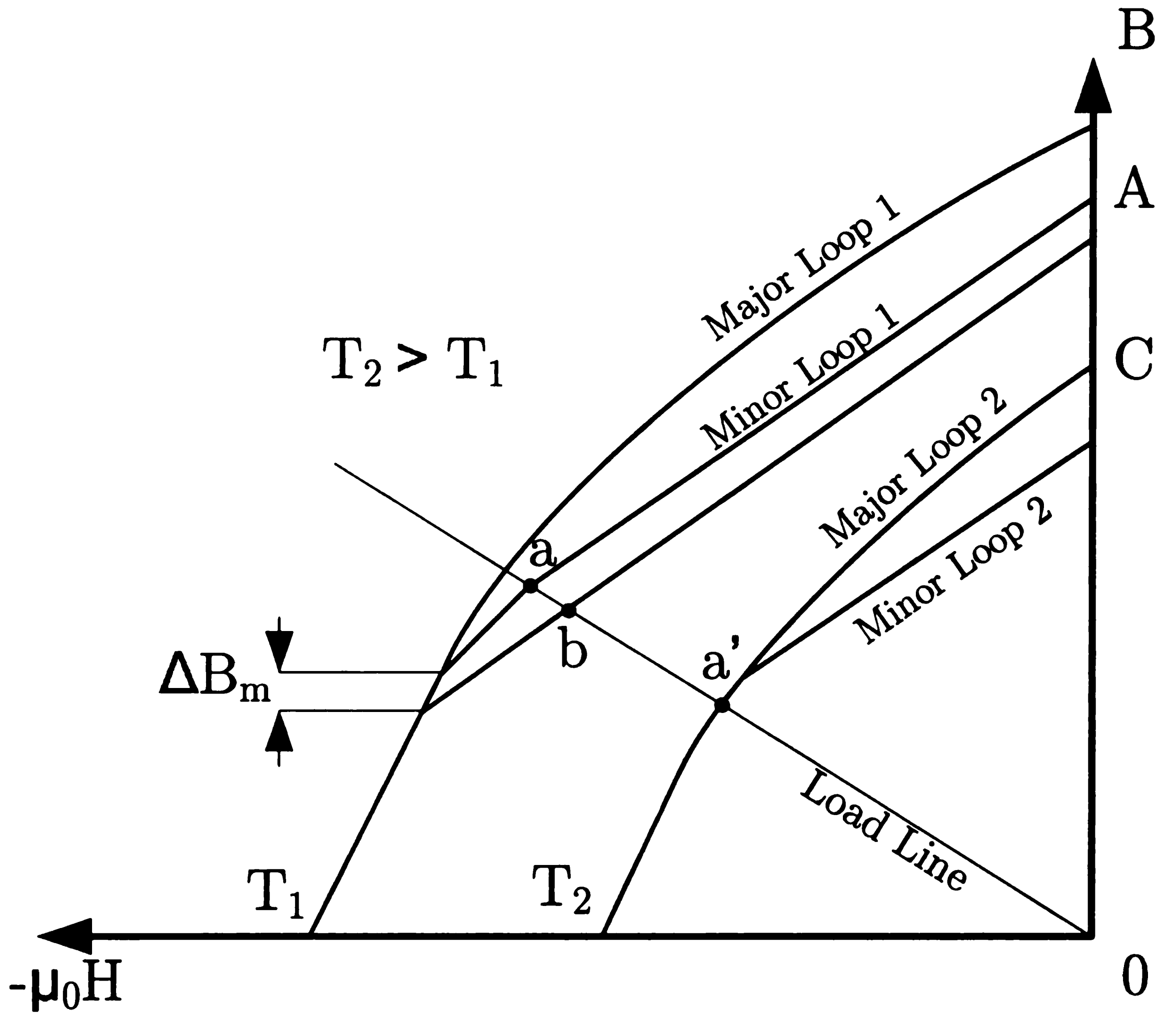

Figure 4.7. Hysteresis Losses Due to Temperature Change

with maximum remanence at point A. As temperature increases from T_1 to T_2, the hysteresis loop shrinks. If the operating point is at the lower end of the curve (near point a), it can slide down to a lower point (point a'). The maximum remanence is less at point a' than at point a, and is represented by point C. If the temperature decreases back to T_1, the operating point will not be able to return to point a. The operating point will move to point b with less flux. Being stuck at operating point b will result in less flux than the previous loop and decrease the performance of the motor. The change in remanence is denoted by ΔB_m. The only way to correct this loss is by re-magnetizing the magnet.

4.5.2 Permanent Magnet Life Model

The lifetime of permanent magnets can be modeled using stress as an aging factor. Magnets lose their effectiveness when their flux decreases. The flux can decrease due to temperature increasing. As noted in Section 4.5.1, the remanence for NdFeB decreases by $0.11\%/°C$. This can be used as the rate of aging for the magnet. As the temperature rises, the flux of the magnet decreases. At a given operating point, there is a certain amount of flux required to operate. If the flux is below this minimum amount, then the magnet can be considered demagnetized. We can assume that if a magnet is no longer able to provide the magnetization necessary for operation, then it is at its end of life. The life of the magnet can be estimated by Equation 4.18.

$$L_{permanent\,magnet} = L_0 * exp(-F * T) \tag{4.18}$$

where,

- $L_{permanent\,magnets}$– quantitative life measurement (hours)
- L_0– quantitative normal life measurement (hours)
- F – the rate of flux decay per degree Celsius (Wb/$°C$)

- ΔT – temperature rise ($°C$)

The failure rate is inverse to the lifetime, L. The failure rate is given by Equation 4.19.

$$\lambda_{permanent\ magnet} = \frac{1}{L_{permanent\ magnet}}. \tag{4.19}$$

Figure 4.8 shows the lifetime predicted by the model in Equation 4.18.

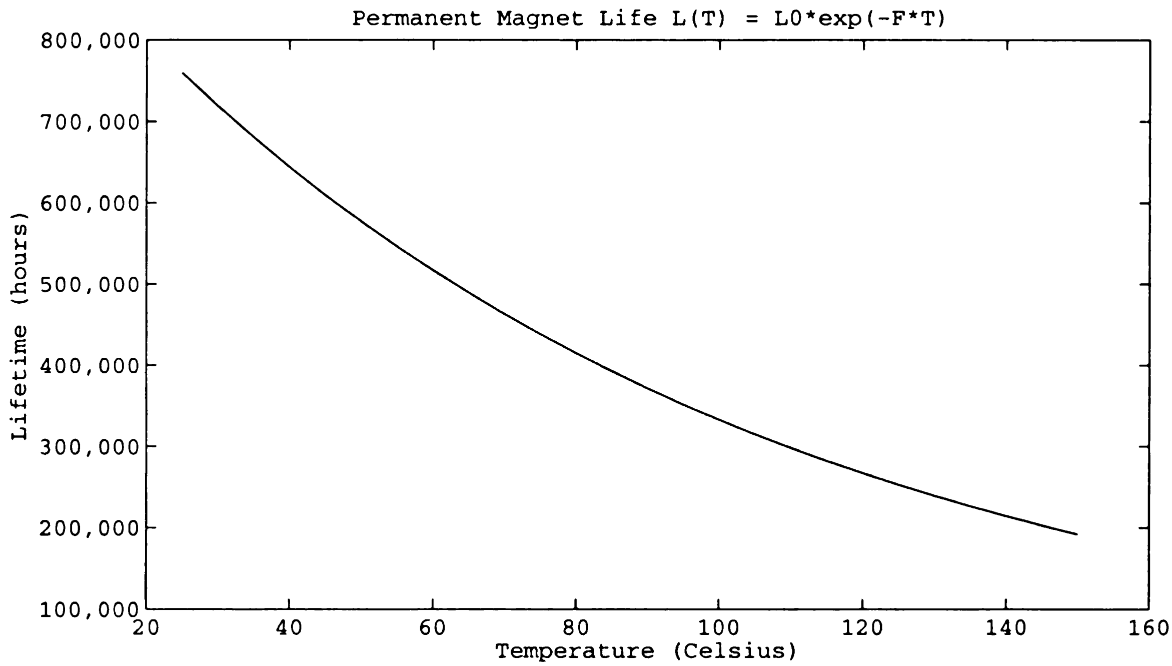

Figure 4.8. Permanent Magnet Life Model

4.6 Modeling Bearing Damage

There are several factors to choosing bearings including machine size, application, and operating environment. Therefore, the use of absolute currents is not applicable. However, using the current density with area based on the contact area between the balls and the bearing walls is more applicable [Mue04]. The bearing current density is defined by Equation 4.20 [Mue04].

$$J_{bearing} = \frac{i_{bearing}}{A_H} \tag{4.20}$$

Experimental results indicate that for DC and low frequency AC (50/60 Hz) [Mue04]:

- $J_{bearing} \leq 0.1 \frac{A}{mm^2}$ are not damaging.
- $J_{bearing} \geq 0.7 \frac{A}{mm^2}$ may reduce bearing life.

For Electrostatic Discharge and high dv/dt currents [Mue04]:

- $J_{bearing} \leq 0.4 \frac{A}{mm^2}$ no effect on life.
- $J_{bearing} \leq 0.6$ - $0.8 \frac{A}{mm^2}$ probably no effect on life.
- $J_{bearing} \geq 0.8 \frac{A}{mm^2}$ may damage bearing.

Since the current density has a direct affect on the life of the bearings, the electrical bearing stress can be considered a function of the current density as denoted by Equation 4.21 [Mue04].

$$W = J_{bearing} \tag{4.21}$$

The life time of bearings can be modeled using the stress factor, W. Using the exponential life model, if a constant stress is applied, the time until failure can be calculated. The exponential life model for bearing current damage is given by Equation 7.15

$$L_{bearing} = L_0 * exp(-W) \tag{4.22}$$

where,

- $L_{bearings}$ – quantitative life measurement (hours)
- L_0 – quantitative normal life measurement (hours)

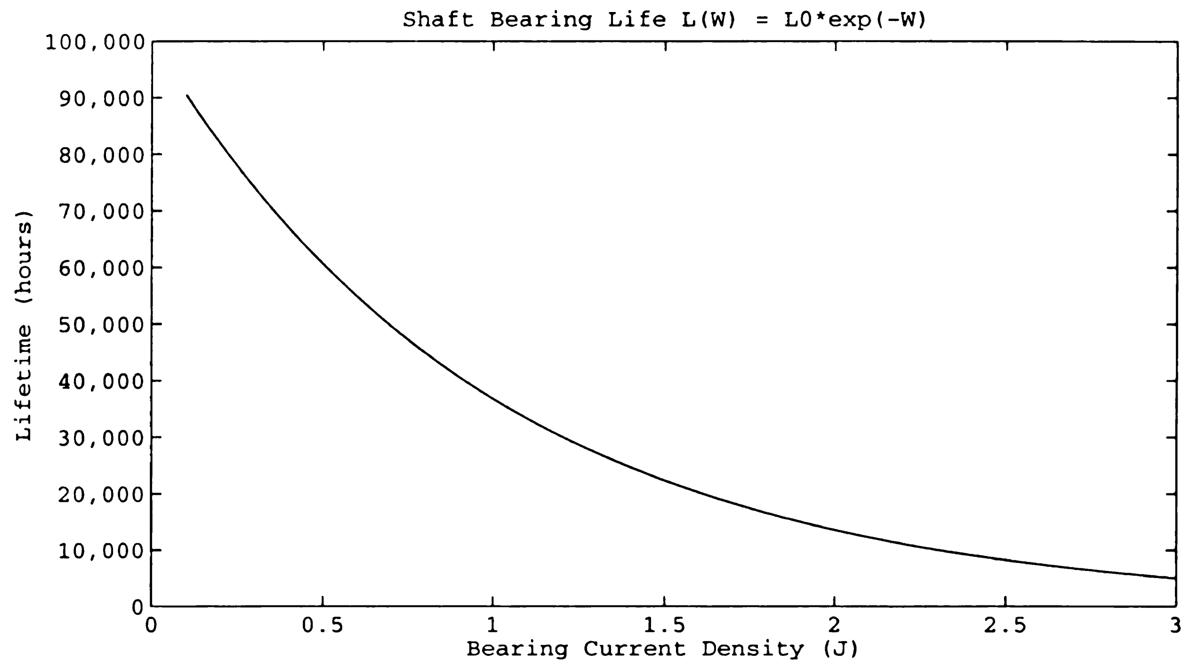

Figure 4.9. Bearing Life

- W – bearing stress defined by Equation 7.16

The inverse of the life model (Equation 4.23) provides the failure rate which will be used for the reliability analysis. Figure 4.9

$$\lambda_{bearing} = \frac{1}{L_{bearing}}. \tag{4.23}$$

CHAPTER 5

Determining System Reliability

5.1 Initial Reliability

In the analysis of PMAC machine reliability, the normal operation reliability is determined using the baseline failure rates of the major components. Figure 5.1 contains a block diagram of the process involving measuring reliability under normal operation after a fault has occurred. There are four areas of consideration in determining the reliability of the controller and motor. A summary of each area and data required for calculation of reliability is provided below.

Semiconductor Reliability Calculation

- The semiconductor reliability calculation is determined based on manufacturer life time data.
- The ambient temperature for approximating the junction temperature.
- The power level at which the switches operate.

Motor Winding Insulation Reliability Calculation

- The motor winding insulation reliability calculation is determined from manufacturer life time data.
- The winding temperature estimated from the power losses in the windings.

Permanent Magnet Reliability Calculation

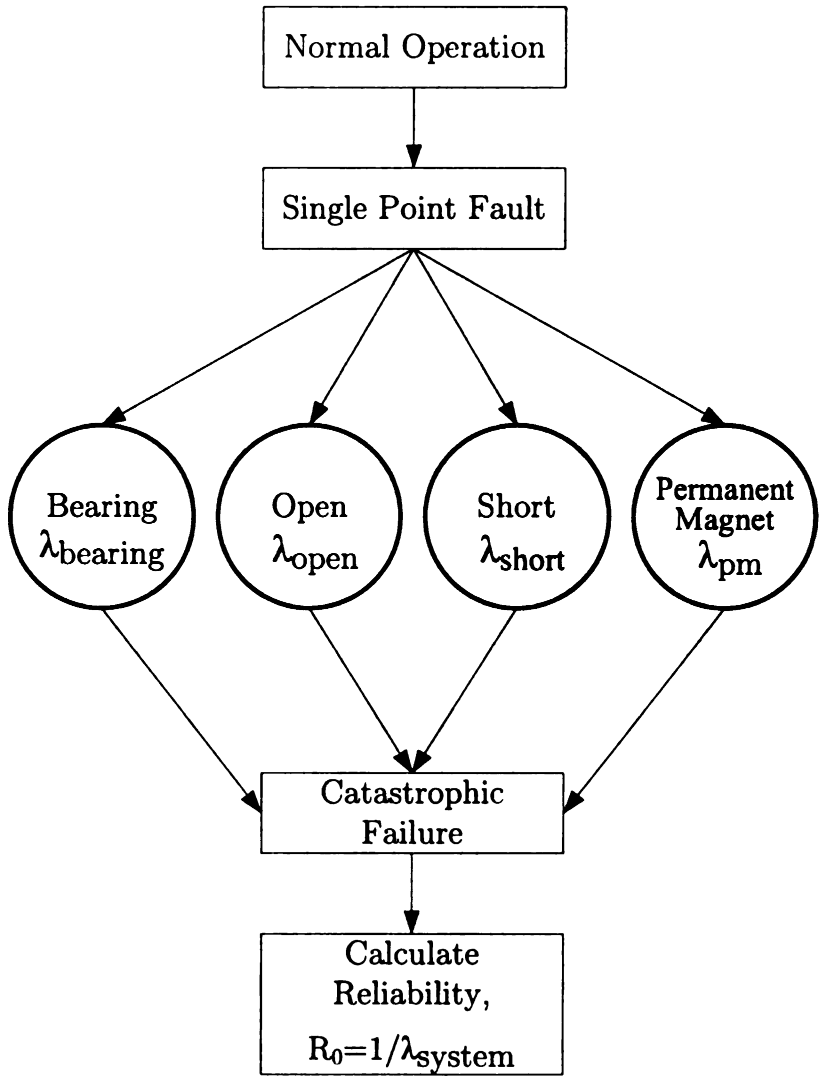

Figure 5.1. Normal Operation Reliability Block Diagram

- The permanent magnet reliability calculation is based on design of the motor.
- The permanent magnets are susceptible to demagnetization as the temperature of the material increases.

Motor Shaft Bearings Reliability Calculation

- The bearing reliability calculation is dependent on the manufacturer life time data.
- The bearings have a significantly increased chance of damage when the bearing current density increases above 1 $\frac{A}{mm^2}$.

5.2 Initial Reliability Calculations

The reliability under normal operation is determined assuming that the controller and motor are operating at room temperature and rated power. The failure rate of each component is determined according to the equations determined in Chapter 4. Each failure rate is calculated and then the summation of each component's failure rate represents the combined failure rate of the motor and controller. The calculations for the device failure rates were performed using Matlab. The code used is provided in Appendix A. The initial reliability is based on the default manufacturer's values at the rated power and temperature. The effects on the permanent magnets and bearing currents can safely be ignored under these conditions due to the assumption that temperature and power are at rated conditions.

5.2.1 Calculation Steps

The failure rate of the individual components is the inverse of the component's Mean Time Between Failures (MTBF) as noted by G.W.A. Dummer *et al.* [DG66]. The diagram in Figure 5.2 illustrates the flow from the individual component failure rates, to the system failure rate, and then to the system MTBF.

$$MTBF = \frac{1}{\lambda} \tag{5.1}$$

$$\lambda = \frac{1}{MTBF} \tag{5.2}$$

The first step is to obtain the failure rate, λ. This is done for each component and results in λ_1 , λ_2 , ..., λ_n for n components. Summing λ_1 through λ_n will result in λ_{system} , the total failure rate of the system.

$$\lambda_{system} = \sum(\lambda_1 + \lambda_2 + ... + \lambda_n) \tag{5.3}$$

The system MTBF is the inverse of the system failure rate, λ_{system} as noted in Equation 5.4.

$$MTBF_{system} = \frac{1}{\lambda_{system}} \tag{5.4}$$

The overall reliability of the motor and controller can be determined based on the MTBF. The larger the MTBF the less chance that there will be failures.

5.3 Remedial Reliability

The next step in the analysis is to determine the effects of different remedial designs either by redesigning the controller and motor or simply changing operation of the system, as outlined in Chapter 4. After a fault has occurred, a corrective action will be taken to clear the fault and keep the motor operational. Depending on the method used to clear the fault, the system parameters will change. These changes will inevitably lead to changes in the reliability of the motor under these new conditions. A block diagram of this process is in Figure 5.3. First faults are denoted by λ and secondary faults are denoted by λ^*. The reliability is determined as the sum of the normal operation lifetime and the remedial operation lifetime.

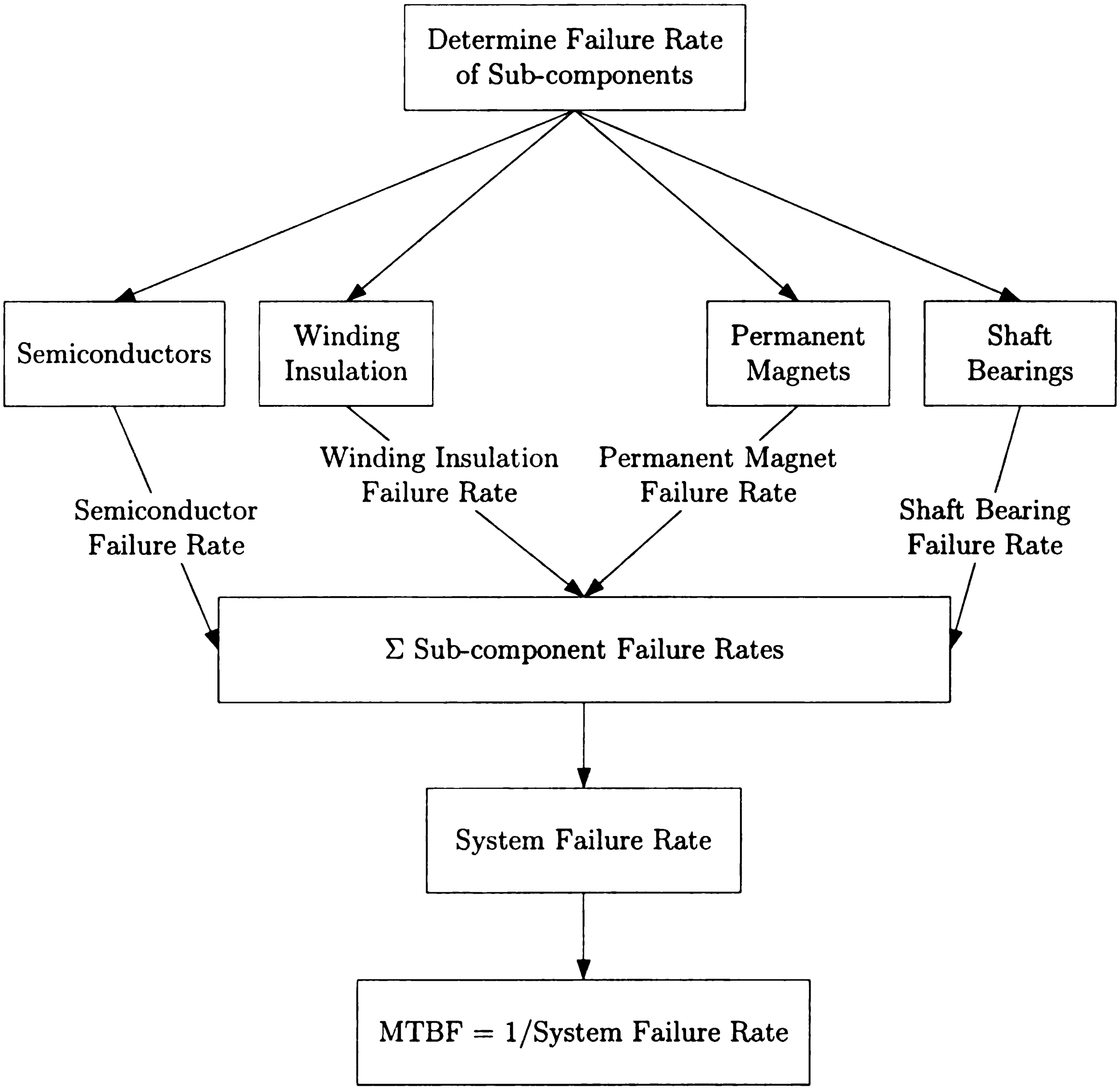

Figure 5.2. Determining System Reliability Through Component Reliability

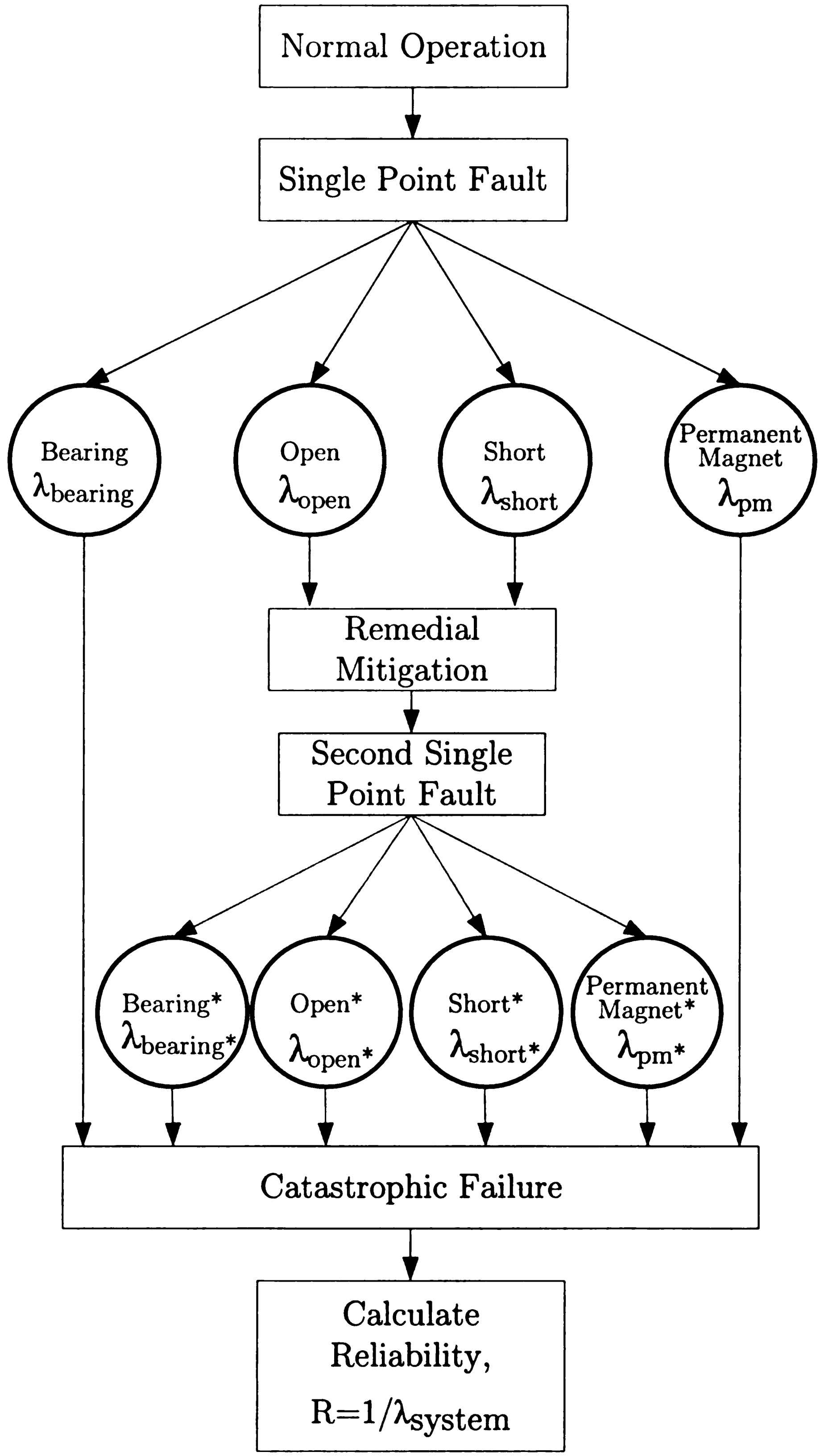

Figure 5.3. Remedial Operation Reliability Block Diagram

5.4 Failure Modes

In the case of a typical three phase drive and motor, any fault can lead to a failure. A state diagram, like Figure 5.4, is useful for outlining the flow from one state to another. In this diagram, the failure rate is denoted by $\lambda_{bearing}$, for a shaft bearing

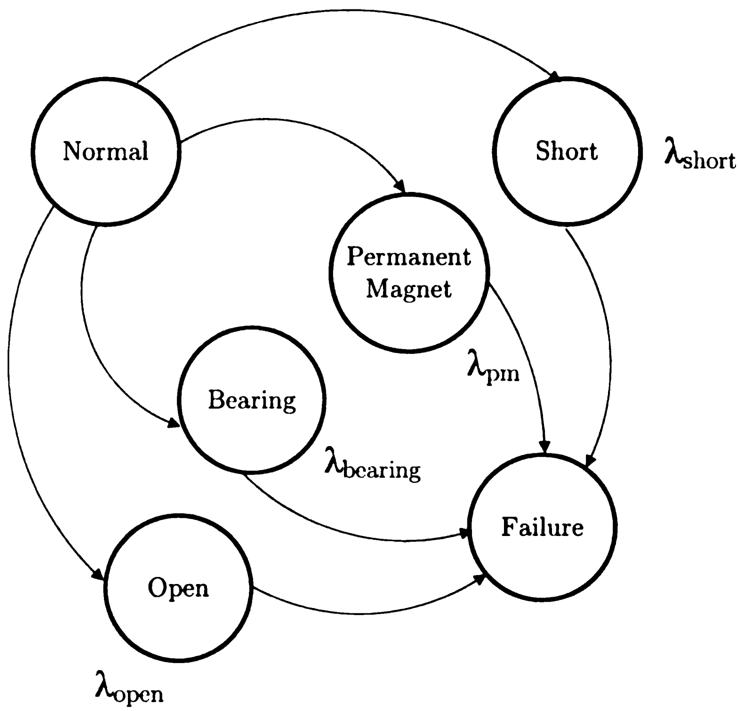

Figure 5.4. Normal Failure States

fault, λ_{open} , for an open circuit fault, λ_{pm} , for permanent magnet fault, and λ_{short} , for a short circuit fault. For more advanced drives that use remedial strategies to overcome faults, this type of state diagram can be modified to aide in determining the probability of failures given what previous failures have occurred. In Figure 5.5, given an open or short fault, failure is not imminent due to the remedial strategy. The state of the machine will move from normal operation to remedial operation. The remedial strategy can stress other components, causing additional secondary

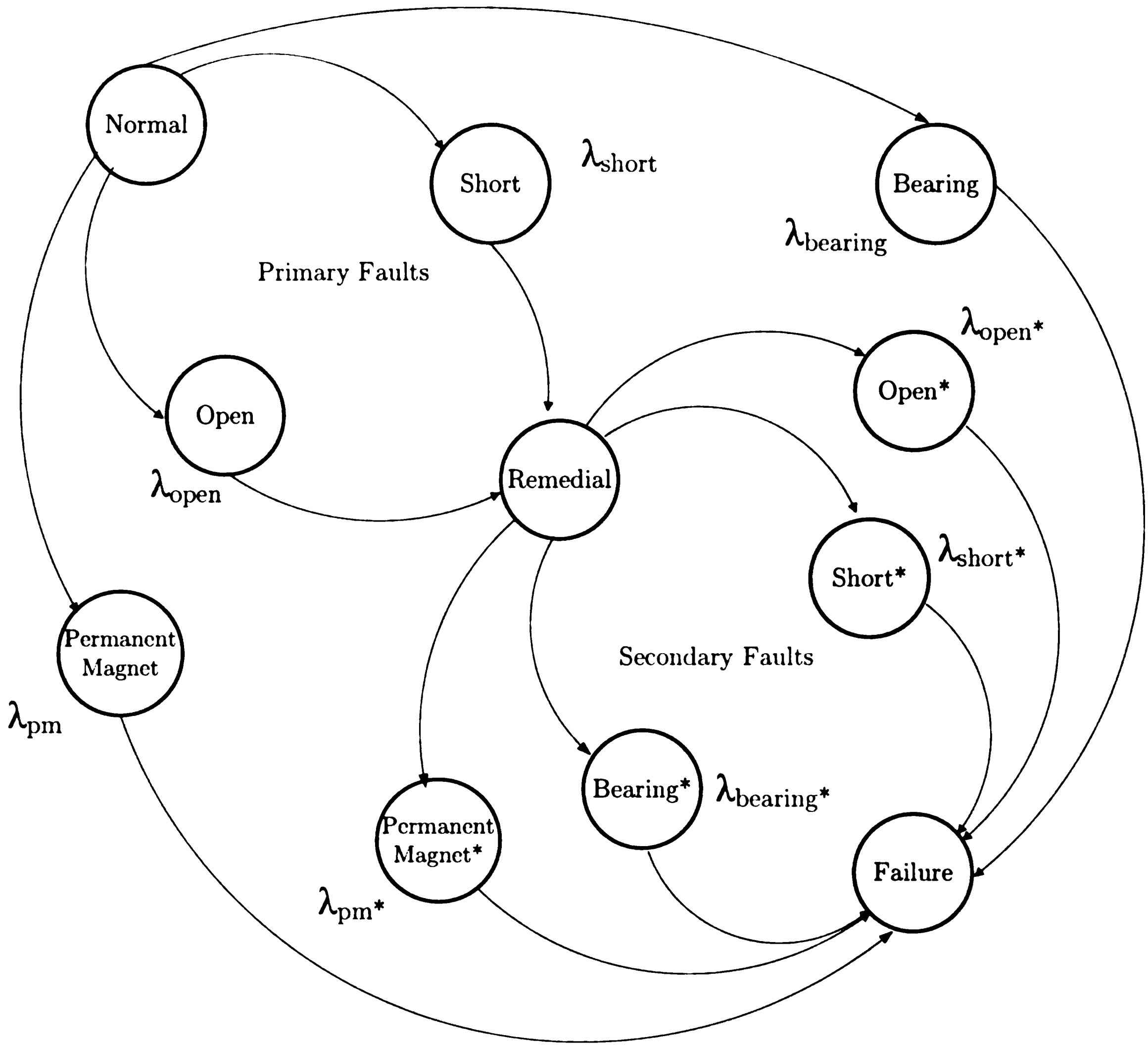

Figure 5.5. Reduced Mode Failure States

failures, which will lead to a catastrophic failure. In Figure 5.5, the starred failures are considered secondary failures that result from a primary fault occurring. Using the state diagram can be useful for determining what faults are most probable, depending on the remedial strategy. J.V. Bukowski *et al.* proposed using state models for determining the MTBF of a system [BG01]. The starred failure rates are dependent on the remedial solution, as different remedial solution will stress components in different ways. For example, given an open fault with a remedial solution of using

$\lambda_{open} = 5{*}10^{-3}$	$\lambda_{short} = 5{*}10^{-3}$
$\lambda_{open*} = 10{*}10^{-3}$	$\lambda_{short*} = 10{*}10^{-3}$
$\lambda_{bearing*} = 5{*}10^{-3}$	$\lambda_{magnet*} = 5{*}10^{-3}$

Table 5.1. State Diagram Failure Rates

a centered tapped DC-bus inverter to correct the fault. The bearing currents may increase, due to unbalanced operation of the two phase mitigation. If the bearing currents surpass a certain threshold, damage could result and eventually lead to bearing failure. The component(s) with the largest λ^* will be most susceptible to failure.

An example is provided in Figure 5.6. Four different system failure rates are possible depending on the path of failure. The four paths of failure: open-open$*$, open-short$*$, open-bearing$*$, or open-magnet$*$. Each failure is preceded by an open fault. The secondary faults, denoted by an asterisk, result from the increased stress of the remedial strategy. Using the failure rates from Table 5.1, the failure rates for each of the four failure path are calculated as follows. It is possible to create a fault tree for any type of failure scenario.

$$\lambda_{open-open^*} = \lambda_{open} + \lambda_{open^*} = 5 * 10^{-3} + 10 * 10^{-3} = 15 * 10^{-3} \tag{5.5}$$

$$\lambda_{open-short^*} = \lambda_{open} + \lambda_{short^*} = 5 * 10^{-3} + 10 * 10^{-3} = 15 * 10^{-3} \tag{5.6}$$

$$\lambda_{open-bearing^*} = \lambda_{open} + \lambda_{bearing^*} = 5 * 10^{-3} + 5 * 10^{-3} = 10 * 10^{-3} \tag{5.7}$$

$$\lambda_{open-magnet^*} = \lambda_{open} + \lambda_{magnet^*} = 5 * 10^{-3} + 5 * 10^{-3} = 10 * 10^{-3} \tag{5.8}$$

$$\lambda_{total} = \lambda_{open-open^*} + \lambda_{open-short^*} + \lambda_{open-bearing^*} + \lambda_{open-magnet^*} = 50 * 10^{-3} \tag{5.9}$$

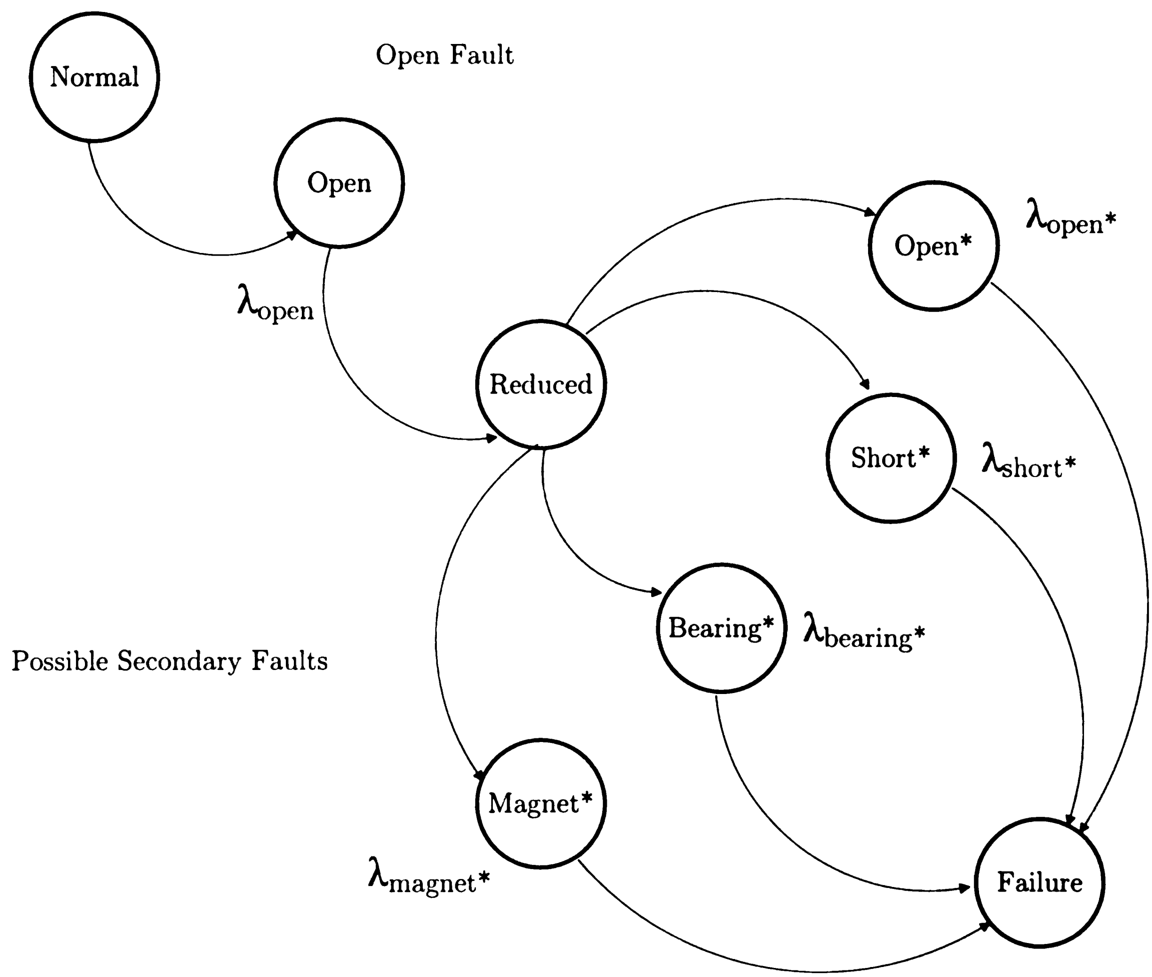

Figure 5.6. Open Fault Failure State Diagram

CHAPTER 6

Normal Operation Reliability

6.1 Normal Lifetime

In this example, the lifetime of the components is determined using estimated lifetimes of the respective component. These lifetimes assume normal operation under which the components do not experience accelerated aging due to stress from current, temperature, voltage, or similar stresses. As discussed in Chapter 5 Section 5.2.1, there are three steps in determining the system failure rate.

1. Determine the component failure rates.

2. Determine the system failure rate.

3. Determine the system MTBF.

6.2 Component Failure Rates

6.2.1 Semiconductors

The lifetime of the semiconductors is determined using Equation 6.1.

$$L_{semiconductor} = L_0 * exp(-B * \Delta T_J) \tag{6.1}$$

where,

- $L_{semiconductor}$ – quantitative life measurement (hours)

- L_0 – quantitative normal life measurement (hours)
- B – $\frac{E_A}{K}$
- ΔT_J – stress (based on junction temperature in Kelvin)

For this analysis, L_0 is chosen as 1,000,000 hours. This corresponds to a failure rate of 1 unit in 1,000,000 hours. Since normal operation is assumed, the lifetime is exactly the normal life expectancy. The failure rate is calculated by Equation 6.2.

$$\lambda_{semiconductor} = \frac{1}{1,000,000} = 1.0 * 10^{-6} \tag{6.2}$$

6.2.2 Winding Insulation

The lifetime of the winding insulation is determined using Equation 6.3.

$$L_{insulation} = L_0 * exp(-B * \Delta T) \tag{6.3}$$

where,

- $L_{insulation}$ – quantitative life measurement (hours)
- L_0 – quantitative normal life measurement (hours)
- B – $\frac{E_A}{K}$
- Δ T – thermal stress defined by Equation 4.16

For this analysis, L_0 is chosen as 100,000 hours. This corresponds to a failure rate of 1 unit in 100,000 hours. Since normal operation is assumed, the lifetime is exactly the normal life expectancy. The failure rate is calculated by Equation 6.4.

$$\lambda_{insulation} = \frac{1}{100,000} = 1.0 * 10^{-5} \tag{6.4}$$

6.2.3 Permanent Magnets

The life of the magnet can be estimated by Equation 7.13.

$$L_{permanent\,magnet} = L_0 * exp(-F * T) \tag{6.5}$$

where,

- $L_{permanent\,magnets}$ – quantitative life measurement (hours)
- L_0 – quantitative normal life measurement (hours)
- F – the rate of flux decay per degree Celsius (Wb/$°C$)
- ΔT – temperature rise ($°C$)

For this analysis, L_0 is chosen as 1,000,000 hours. This corresponds to a failure rate of 1 unit in 1,000,000 hours. Since normal operation is assumed, the lifetime is exactly the normal life expectancy. The failure rate is calculated by Equation 6.6.

$$\lambda_{permanent\,magnet} = \frac{1}{1,000,000} = 1.0 * 10^{-6} \tag{6.6}$$

6.2.4 Shaft Bearings

The exponential life model for bearing current damage is given by Equation 6.7

$$L_{bearing} = L_0 * exp(-W) \tag{6.7}$$

where,

- $L_{bearings}$ – quantitative life measurement (hours)
- L_0 – quantitative normal life measurement (hours)

- W – bearing stress defined by Equation 7.16

$$W = J_{bearing} \tag{6.8}$$

For this analysis, L_0 is chosen as 100,000 hours. This corresponds to a failure rate of 1 unit in 100,000 hours. Since normal operation is assumed, the lifetime is exactly the normal life expectancy. The failure rate is calculated by Equation 6.9.

$$\lambda_{bearing} = \frac{1}{100,000} = 1.0 * 10^{-5} \tag{6.9}$$

6.3 Normal System Failure Rate

The system failure rate is calculated by summing up the individual failure rates of the independent faults using Equation 6.10. Replacing $\lambda_{semiconductors}$, $\lambda_{insulation}$, $\lambda_{permanent\, magnets}$, and $\lambda_{bearings}$with the failure rates of the semiconductors and winding insulation results in Equation 6.11.

$$\lambda_{system} = \sum(\lambda_{semiconductor} + \lambda_{insulation} + \lambda_{permanent\, magnets} + \lambda_{bearings}) \tag{6.10}$$

$$\lambda_{system} = \sum(1.0 * 10^{-6} + 1.0 * 10^{-5} + 1.0 * 10^{-6} + 1.0 * 10^{-5}) = 2.2 * 10^{-5} \tag{6.11}$$

The system failure rate is the inverse of the system MTBF, which is the expected lifetime of the system in hours. The system MTBF is given in Equation 6.12.

$$MTBF_{system} = \frac{1}{2.2 * 10^{-5}} \approx 45,455\, hours \tag{6.12}$$

CHAPTER 7

Reliability of a System with Remediation

This analysis will examine two example cases of fault remedies and their respective reliability. Using the methods described in the previous chapter on reliability, the failure rates will be calculated for the semiconductors, winding insulation, permanent magnets, and shaft bearings. A comparison will be done between normal operation and the two remedial examples.

7.1 Centered Tapped DC-bus Operation

The first case deals with an open fault in phase a of the motor. The remedial solution adjusts by increasing currents in the remaining healthy phases. The magnitude of the current in phase b and c will be increased to $\sqrt{3}$ and the phase of each current shifted to $\pi/3$, as described in Chapter 3 Section 3.1. The next step in this analysis is to re-evaluate the reliability under the new operating conditions. Unlike the normal operation reliability, this calculation will include the effects of the physical and environmental stress, resulting from the change in operation.

7.1.1 Semiconductor Failure Rate

Assuming normal operation was at 33% of the power rating of the switches, then the new power rating (Equation 7.1) would be the magnitude increase, $\sqrt{3}$, multiplied by the power rating.

$$P_{rating} = 0.33 * \sqrt{3} = 0.57pu \tag{7.1}$$

The new power rating, P_{rating}, can be substituted for P_D in Equation 7.2 to calculate the junction temperature at the new power level. The ambient temperature is assumed to be room temperature (T_A=25 °C). The thermal resistance, Θ_{JA}, is assumed to be 62 °C/W.

$$T_J = T_A + P_D\Theta_{JA} = 25 + 0.57 * 62 \approx 60°C \tag{7.2}$$

where,

- T_J – junction temperature (°C)
- T_A – ambient temperature (°C)
- P_D – average power dissipated by device (W)
- Θ_{JA} – thermal resistance from junction to ambient (°C/W)

The life time is then calculated using Equation 7.3.

$$L_{semiconductor}(T_J) = L_0 * exp(-B * \Delta T_J) = 1 * 10^6 * exp(-1160 * 3.5 * 10^{-4}) \approx 661,765 \tag{7.3}$$

where,

- $L_{semiconductor}$ – quantitative life measurement (hours)
- L_0 – quantitative normal life measurement (hours)
- B – $\frac{E_A}{K}$ defined by Equation 7.4
- ΔT_J – thermal stress defined by Equation 7.5

$$B = \frac{E_A}{K} = \frac{0.1}{8.617385 * 10^{-5}} \approx 1160 \tag{7.4}$$

where,

- E_A – activation energy
- K – Boltzman's constant

$$\Delta T = \frac{1}{T_A} - \frac{1}{T} = \frac{1}{298} - \frac{1}{333} = 3.5 * 10^{-4} \tag{7.5}$$

where,

- T_A – the ambient temperature (Kelvin)
- T – component temperature (Kelvin)

The inverse of the lifetime provides the failure rate of the semiconductor device as defined by Equation 7.6.

$$\lambda_{semiconductor} = \frac{1}{661,765} \approx 1.51 * 10^{-6} \tag{7.6}$$

7.1.2 Winding Insulation Failure Rate

Since the current in the healthy phases has increased to $\sqrt{3}$, the winding losses have also increased. The increase in power is proportional to the temperature rise increase, and therefore the increase in the winding temperature can be estimated. The new winding temperature will be used to determine the lifetime of the winding insulation. The first step is to determine the change in the losses. Using Equation 7.7, the change in power between normal operation and using a centered tapped DC-bus can be calculated.

$$P_{losses} = \frac{(n-1) * |\sqrt{3}|^2 * R}{n * |I|^2 * R} = \frac{2 * |3| * 0.1}{3 * |1|^2 * 0.1} = 2 \tag{7.7}$$

Assuming normal operation was at room temperature, then the rise in temperature is T_{room}. The new temperature rise using a centered tapped DC-bus, T_{rise}, can be estimated using Equation 7.8.

$$T_{rise} \approx T_{room} * P_{losses} \approx 25 * 2 \approx 50°C \tag{7.8}$$

Using T_{rise} and Equation 7.9 the insulation lifetime can be modeled.

$$L_{insulation} = L_0 * exp(-B * \Delta T) = 1 * 10^5 * exp(-1160 * 2.6 * 10^{-4}) \approx 73,978 \tag{7.9}$$

where,

- $L_{insulation}$ – quantitative life measurement (hours)
- L_0 – quantitative normal life measurement (hours)
- B – $\frac{E_A}{K}$ by Equation 7.10
- Δ T – thermal stress defined by Equation 7.11

$$B = \frac{E_A}{K} = \frac{0.1}{8.617385 * 10^{-5}} \approx 1160 \tag{7.10}$$

where,

- E_A – activation energy
- K – Boltzman's constant

$$\Delta T = \frac{1}{T_A} - \frac{1}{T} = \frac{1}{298} - \frac{1}{323} = 2.6 * 10^{-6} \tag{7.11}$$

where,

- T_A – the ambient temperature (Kelvin)
- T – component temperature (Kelvin)

The failure rate is inverse to the lifetime, L. The failure rate is described by Equation 7.12.

$$\lambda_{insulation} = \frac{1}{73,978} \approx 1.35 * 10^{-5} \tag{7.12}$$

7.1.3 Effects on Permanent Magnets

As noted in Chapter 4 Section 4.5, NdFeB permanent magnets are susceptible to magnetization loss when the motor is not operated under reliable flux density. Using a centered tapped DC-bus inverter, the phase currents are $\sqrt{3}$ times larger than normal operation. This results in an increase in the temperature rise by a factor of two. As the temperature of the magnets rise, the hysteresis loop shrinks decreasing the flux density.

In Figure 7.1, as the temperature increases the flux required for normal operation is not obtainable due to the hysteresis loop shrinking. If the temperature continues to increase, it is possible to further weaken and damage the magnets. During a fault, the temperature may rise to T_2 due to increase losses resulting from increased stator currents. At T_2, the operating point falls off the recoil line. When the fault is cleared, the temperature may decrease back to T_1. However, instead of returning to the original recoil line corresponding to T_1, the new operating point will be on a recoil line denoted by the dash–dot–dash line in Figure 7.1. The flux at this point will be less than the previous flux capable at T_1 (denoted by the solid black recoil line) prior to the fault. Any additional temperature increases may move the operating point further down the load line decreasing the flux even more. It is important to understand the effects of temperature on the permanent magnets so that if a fault does occur, any recovery technique does not cause additional faults that may damage the magnets.

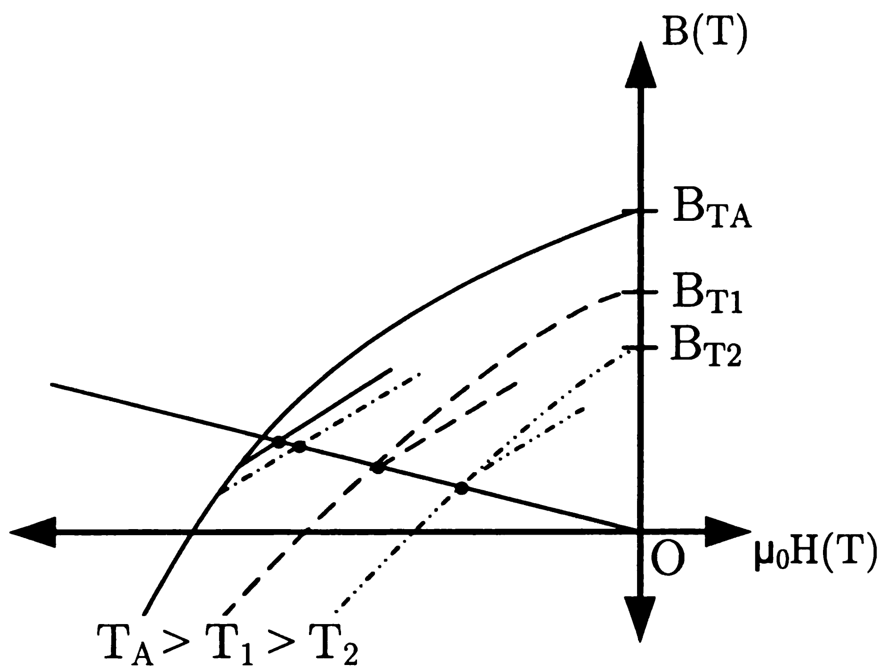

Figure 7.1. Centered Tapped DC-bus: Temperature Effects on Hysteresis Loop

The temperature of the magnets can be estimated from the winding power losses, as defined by Equation 7.8. The life model is given by Equation 7.13.

$$L_{permanent\,magnet} = L_0 * exp(-F * \Delta T) = 1 * 10^6 * exp(-0.011 * 50) = 576,950 \quad (7.13)$$

where,

- $L_{permanent\,magnets}$ – quantitative life measurement (hours)

- L_0 -- quantitative normal life measurement (hours)

- F – the rate of flux decay per degree Celsius (Wb/$^\circ C$)

- ΔT – temperature rise ($^\circ C$)

The failure rate is inverse to the lifetime, $L_{permanent\, magnet}$, and is described by Equation 7.14.

$$\lambda_{permanent\, magnet} = \frac{1}{576,950} \approx 1.73 * 10^{-6} \tag{7.14}$$

7.1.4 Effects on Bearings

Under the proposed remedial solution, instead of three phases, only two phases are used to control the motor. Using the same simulation setup from Chapter 2 Section 2.2.2, phase a was disconnected from the inverter. The PWM common mode voltage that resulted is $\frac{\sqrt{3}}{6}V_{dc}$ and is $\sqrt{3}$ times larger than the PWM common mode voltage under three phase operation. In Figure 7.2, part (a) is a graph of the two phase PWM source and part (b) is the common mode voltage. By changing from three phase to using a centered tapped DC-bus inverter, there is approximately a 73% increase in the common mode voltage. Since the bearing voltage is proportional to the common mode voltage, it is probable that the bearing voltage will increase as well, causing the bearing current to increase. It was noted Chapter 4 Section 4.6 that bearing currents are not practical for determining damage to a bearing, however current densities are more applicable. Using the experimental results from Chapter 4 Section 4.6 and multiplying by $\sqrt{3}$ results in the following bearing current densities that can be used for the centered tapped DC-bus inverter.

Electrostatic Discharge and high dv/dt currents:

- $J_{bearing} \leq 0.69\ \frac{A}{mm^2}$ no effect on life.

- $J_{bearing} \leq 1.0$ - $1.39\ \frac{A}{mm^2}$ probably no effect on life.

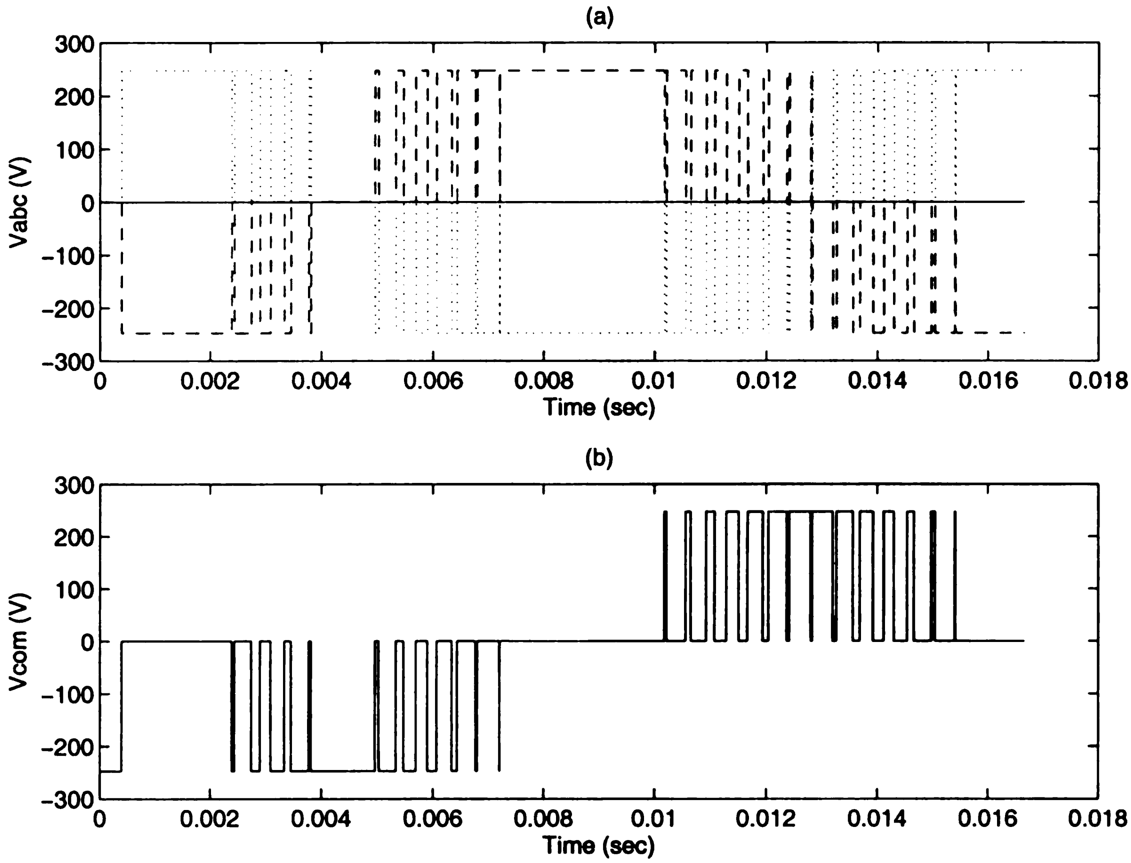

Figure 7.2. PWM and Common Mode Voltages Using a Centered Tapped DC-bus Inverter Simulation Results: (a) 230V PWM Source, (b) Common Mode Voltage

- $J_{bearing} \geq 1.39 \frac{A}{mm^2}$ may damage bearing.

The exponential life model for bearing current damage is given by Equation 7.15

$$L_{bearings} = L_0 * exp(-W) = 1 * 10^5 * exp(-1.73) \approx 17,692 \quad (7.15)$$

where,

- $L_{bearings}$ – quantitative life measurement (hours)
- L_0 – quantitative normal life measurement (hours)
- W – bearing stress defined by Equation 7.16

$$W = J_{bearing} = 1.0 * \sqrt{3} \approx 1.73 \quad (7.16)$$

The failure rate is inverse to the lifetime, $L_{bearing}$, and is described by Equation 7.37.

$$\lambda_{bearing} = \frac{1}{L_{bearing}} = \frac{1}{17,692} \approx 5.65 * 10^{-5} \quad (7.17)$$

7.1.5 Centered Tapped DC-bus System Failure Rate

The system failure rate is calculated by summing up the individual failure rates of the components under normal operation and using a centered tapped DC-bus inverter. The normal operation system failure rate was calculated in Section 6.3 and is given by Equation 7.18 and Equation 7.19.

$$\lambda_{system-normal} = \sum(\lambda_{semiconductor} + \lambda_{insulation} + \lambda_{permanent\ magnets} + \lambda_{bearings}) \quad (7.18)$$

$$\lambda_{system-normal} = \sum(1.0*10^{-6}+1.0*10^{-5}+1.0*10^{-6}+1.0*10^{-5}) = 2.2*10^{-5} \quad (7.19)$$

The centered tapped DC-bus system failure rate is given by replacing the failure rates in Equation 7.18 with $\lambda_{semiconductors-reduced}$, $\lambda_{insulation-reduced}$, $\lambda_{permanent\ magnets-reduced}$, and $\lambda_{bearings-reduced}$, which results is Equation 7.20.

$$\lambda_{system-center-tapped} = \sum(1.51{*}10^{-6}{+}1.35{*}10^{-5}{+}1.73{*}10^{-6}{+}5.65{*}10^{-5}) = 7.32{*}10^{-5} \tag{7.20}$$

The total system reduced MTBF is the sum of the inverses of the normal and centered tapped DC-bus failure rates, which is the expected lifetime of the system in hours. The total system reduced MTBF is given in Equation 7.21 and 7.22.

$$MTBF_{total-system-center-tapped} = \frac{1}{\lambda_{system-normal}} + \frac{1}{\lambda_{system-center-tapped}} \tag{7.21}$$

$$MTBF_{total-system-center-tapped} = \frac{1}{2.2 * 10^{-5}} + \frac{1}{7.32 * 10^{-5}} \approx 59,100\ hours \tag{7.22}$$

7.2 Redundant Hardware

The second case deals with an open fault in phase a of the motor. The remedial solution switches in a redundant phase leg to replace the damaged phase. The magnitude of current in phase b and c will be increased to $\sqrt{3}$. The current in the redundant phase will be 3 times the rated current because this phase is connected to the neutral point of the motor. The reliability will be calculated under the new operating conditions. Unlike the normal reliability, this calculation will include the effects on the magnets and bearings of the motor as they may be outside their operating range and susceptible to damage that may result in reduced life.

7.2.1 Semiconductor Failure Rate

Assuming normal operation was at 33% of the power rating of the switches, then the new power rating would be the magnitude increase, 3, multiplied by the power rating.

$$P_{rating} = 0.33 * 3 \approx 1.0pu \tag{7.23}$$

The new power rating, P_{rating}, can be substituted for P_D in Equation 7.24 to calculate the junction temperature at the new power level. The ambient temperature will be assumed to be room temperature (T_A=25 °C).

$$T_J = T_A + P_D \Theta_{JA} = 25 + 1.0 * 62 = 87°C \tag{7.24}$$

where,

- T_J – junction temperature (°C)
- T_A – ambient temperature (°C)
- P_D – average power dissipated by device (W)
- Θ_{JA} – thermal resistance from junction to ambient (°C/W)

The life time is then calculated using Equation 7.25.

$$L_{semiconductor}(T_J) = L_0 * exp(-B * \Delta T_J) = 1 * 10^6 * exp(-1160 * 5.7 * 10^{-5}) = 511,375 \tag{7.25}$$

where,

- $L_{semiconductor}$ – quantitative life measurement (hours)
- L_0 – quantitative normal life measurement (hours)
- B – $\frac{E_A}{K}$ defined by Equation 7.26

- ΔT_J – thermal stress defined by Equation 7.27

$$B = \frac{E_A}{K} = \frac{0.1}{8.617385 * 10^{-5}} \approx 1160 \tag{7.26}$$

where,

- E_A – activation energy
- K – Boltzman's constant

$$\Delta T = \frac{1}{T_A} - \frac{1}{T} = \frac{1}{298} - \frac{1}{360} = 5.78 * 10^{-4} \tag{7.27}$$

where,

- T_A – the ambient temperature (Kelvin)
- T – component temperature (Kelvin)

The inverse of the lifetime provides the failure rate of the semiconductor device as defined by Equation 7.28.

$$\lambda_{semiconductor} = \frac{1}{511,375} \approx 1.96 * 10^{-6} \tag{7.28}$$

7.2.2 Winding Insulation Failure Rate

Since the current in the healthy phases has increased to 3 times rated, the winding losses have also increased. The increase in power is proportional to the temperature rise increase, and therefore the increase in the winding temperature can be estimated. The new winding temperature will be used to determine the lifetime of the winding insulation. The first step is to determine the change in the losses. Using Equation 7.29, the change in power between normal operation and redundant hardware operation can be calculated.

$$P_{losses} = \frac{(n) * |3|^2 * R}{n * |I|^2 * R} = \frac{2 * |3|^2 * 0.1}{3 * |1|^2 * 0.1} = 6 \tag{7.29}$$

Assuming normal operation was at room temperature, then the rise in temperature is T_{room}. The new temperature rise under redundant hardware operation, T_{rise}, can be estimated using Equation 7.30.

$$T_{rise} \approx T_{room-rise} * P_{losses} \approx 25 * 6 \approx 150°C \tag{7.30}$$

Using T_{rise} and Equation 7.31 the insulation lifetime can be modeled.

$$L_{insulation} = L_0 * exp(-B * \Delta T) = 1 * 10^5 * exp(-1160 * 9.9 * 10^{-4}) = 31,640 \tag{7.31}$$

where,

- $L_{insulation}$ – quantitative life measurement (hours)
- L_0 – quantitative normal life measurement (hours)
- B – $\frac{E_A}{K}$ defined by Equation 7.32
- Δ T – thermal stress defined by Equation 7.33

$$B = \frac{E_A}{K} = \frac{0.1}{8.617385 * 10^{-5}} \approx 1160 \tag{7.32}$$

where,

- E_A – activation energy
- K – Boltzman's constant

$$\Delta T = \frac{1}{T_A} - \frac{1}{T} = \frac{1}{298} - \frac{1}{423} = 9.92 * 10^{-4} \tag{7.33}$$

where,

- T_A – the ambient temperature (Kelvin)
- T – component temperature (Kelvin)

The failure rate is inverse to the lifetime, $L_{insulation}$. The failure rate is described by Equation 7.34.

$$\lambda_{insulation} = \frac{1}{31,640} \approx 3.16 * 10^{-5} \tag{7.34}$$

7.2.3 Effects on Permanent Magnets

As noted in Chapter 4 Section 4.5, NdFeB permanent magnets are susceptible to magnetic losses when the motor is not operated under reliable flux density. Under redundant hardware operation, the phase currents are three times larger than normal operation. This results in an increase in the temperature rise by a factor of six. As the temperature of the magnets rise, the hysteresis loop shrinks decreasing the flux density.

The effects of temperature increases due to faults was discussed in Section 7.1.3. As noted, any additional temperature increases may move the operating point further down the load line decreasing the flux even more. It is important to understand the effects of temperature on the permanent magnets so that if a fault does occur, any recovery technique does not cause additional faults that may damage the magnets.

The temperature of the magnets can be estimated from the winding power losses, as defined by Equation 7.30. The life model is given by Equation 7.35.

$$L_{permanent\ magnet} = L_0 * exp(-F * \Delta T) = 1 * 10^6 * exp(-0.011 * 150) = 192,050 \tag{7.35}$$

where,

- $L_{permanent\,magnets}$ – quantitative life measurement (hours)
- L_0 – quantitative normal life measurement (hours)
- F – the rate of flux decay per degree Celsius (Wb/$°C$)
- ΔT – temperature rise ($°C$)

The failure rate is inverse to the lifetime, $L_{permanent\,magnet}$, and is described by Equation 7.36.

$$\lambda_{permanent\,magnet} = \frac{1}{192,050} \approx 5.21 * 10^{-5} \tag{7.36}$$

7.2.4 Effects on Bearings

As discussed in Chapter 2 Section 2.2.2, the shaft voltage and bearing voltage are proportional to the common mode voltage. The simulation results from Chapter 2 Section 2.2.2 indicate that PWM inverters create a significant common mode voltage. In the case of a three phase load, the common mode voltage was $\frac{1}{6}V_{dc}$. Under the proposed remedial solution, three phase operation is maintained to control the motor. As the simulation results indicate, even with phase currents increased by three times, the common mode voltage remains the same and there is no increased chance of bearing current damage. The failure rate is inverse to the lifetime, $L_{bearing}$, and is described by Equation 7.37.

$$\lambda_{bearing} = \frac{1}{L_{bearing}} = \frac{1}{100,000} \approx 1 * 10^{-5} \tag{7.37}$$

7.2.5 Redundant Hardware System Failure Rate

The system failure rate using redundant hardware is calculated by summing up the individual failure rates of the components under normal operation and while using redundant hardware. The normal operation system failure rate was calculated in Section 6.3 and is given by Equation 7.38 and Equation 7.39.

$$\lambda_{system-normal} = \sum(\lambda_{semiconductor} + \lambda_{insulation} + \lambda_{permanent\ magnets} + \lambda_{bearings}) \quad (7.38)$$

$$\lambda_{system-normal} = \sum(1.0*10^{-6}+1.0*10^{-5}+1.0*10^{-6}+1.0*10^{-5}) = 2.2*10^{-5} \quad (7.39)$$

The redundant hardware system failure rate is given by replacing the failure rates in Equation 7.38 with $\lambda_{semiconductors-redundant}$, $\lambda_{insulation-redundant}$, $\lambda_{permanent\ magnets-redundant}$, and $\lambda_{bearings-redundant}$, which results is Equation 7.40.

$$\lambda_{system-redundant} = \sum(1.96*10^{-6}+3.16*10^{-5}+5.21*10^{-6}+1.0*10^{-5}) = 4.88*10^{-5} \quad (7.40)$$

The total system redundant hardware MTBF is the sum of the inverses of the normal and redundant hardware failure rates, which is the expected lifetime of the system in hours. The total system redundant hawdware MTBF is given in Equation 7.41 and 7.42.

$$MTBF_{total-system-redundant} = \frac{1}{\lambda_{system-normal}} + \frac{1}{\lambda_{system-redundant}} \quad (7.41)$$

$$MTBF_{total-system-redundant} = \frac{1}{2.2*10^{-5}} + \frac{1}{4.88*10^{-5}} \approx 65,960\ hours \quad (7.42)$$

7.3 Results

The life model calculations were done for normal, centered tapped DC-bus operation, and redundant hardware configurations. The values in Table 7.2 represent the estimated lifetime in hours of the system components under their respective operation.

The estimated system lifetimes are presented in Table 7.3 along with the percent increase, which is the percent difference between the remedial cases compared to the normal case. As seen from the results, systems that employ mitigation offer a significant increase in the lifetime of a standard three phase machine and drive. However, systems capable of operating under mitigation must be rated to handle higher currents and temperatures. These two factors tend to result in higher costs for systems that are capable of fault mitigation.

Normal	Centered Tapped DC-bus	Redundant H/W
$\lambda_{semi} = 1.0*10^{-6}$	$\lambda_{semi} = 1.51*10^{-6}$	$\lambda_{semi} = 1.96*10^{-6}$
$\lambda_{windings} = 1.0*10^{-5}$	$\lambda_{windings} = 1.35*10^{-5}$	$\lambda_{windings} = 3.16*10^{-5}$
$\lambda_{pm} = 1.0*10^{-6}$	$\lambda_{pm} = 1.73*10^{-6}$	$\lambda_{pm} = 5.21*10^{-6}$
$\lambda_{bearing} = 1.0*10^{-5}$	$\lambda_{bearing} = 5.65*10^{-5}$	$\lambda_{bearing} = 1.0*10^{-5}$

Table 7.1. Component Failure Rates

Normal	Centered Tapped DC-bus	Redundant H/W
$MTBF_{semi}$ = 1,000,000	$MTBF_{semi}$ = 1,661,765	$MTBF_{semi}$ = 1,511,375
$MTBF_{windings}$ = 100,000	$MTBF_{windings}$ = 173,978	$MTBF_{windings}$ = 120,932
$MTBF_{pm}$ = 1,000,000	$MTBF_{pm}$ = 1,576,950	$MTBF_{pm}$ = 1,084,163
$MTBF_{bearing}$ = 100,000	$MTBF_{bearing}$ = 117,692	$MTBF_{bearing}$ = 200,000

Table 7.2. Component MTBF (hours)

$MTBF_{normal}$ = 45,455	$Percent_{increase}$ = 0 %
$MTBF_{centered\ tapped\ DC-bus}$ = 51,900	$Percent_{increase}$ = 30.02 %
$MTBF_{redundant-h/w}$ = 65,960	$Percent_{increase}$ = 45.11 %

Table 7.3. System MTBF (hours)

CHAPTER 8

Conclusion

The objective of this work was to examine a Permanent Magnet AC machine and develop an algorithm for determining the reliability during normal operation and remedial operation. This was accomplished by identifying the most common faults and the critical areas of the drive and machine that have an effect on the reliability. For each area, a model was developed to estimate the life time given environmental and physical stresses. Remedial solutions were presented and two were analyzed for their effect on life after a fault.

The reliability algorithm was applied to the centered tapped DC-bus operation and redundant hardware mitigation solutions. Each case was analyzed and results were presented.

In the case of the centered tapped DC-bus operation, power was increased in the two healthy phases, which allowed for continued operation with minimal impact on performance. The side effects were increased current, increased winding temperature, and unbalanced operation. Secondary effects led to increased permanent magnet temperature and increased bearing currents. Using centered tapped DC-bus operation, the lifetime was increased by approximately 30%.

In the case of the redundant hardware, power was increased in the two healthy phases and a fourth phase leg was connected to the neutral point of the motor, which allowed for continued operation with minimal impact on performance. The side effects of the current increase was an increase in winding temperature. Secondary effects led to increased permanent magnet temperature. Using redundant hardware increased life by 45%.

Using the reliability algorithm along with the failure state flowcharts, it is possible to identify failures in a design prior to operation leading to more robust systems. In addition to determining normal operation failures, typical remedial solutions are also included to provide an estimate lifetime during mitigated operation. Providing both normal and mitigation reliability makes this a useful analysis/design tool.

Additional research into more detailed reliability models could result in more accurate lifetime estimates. The benefit of more detailed models is that they could account for additional stresses.

Finally, future work could expand the reliability models to include additional machines, and the algorithm could be expanded to include more faults and remedial solutions.

APPENDICES

APPENDIX A

Appendix A

```
%%%%%%%%%%%%%%%%%%%%%%%%%%%%%%%%%%%%%
% PM Motor Reliability Calculations %
% John Neely                        %
%%%%%%%%%%%%%%%%%%%%%%%%%%%%%%%%%%%%%
close all                     % Close open windows
format short g;
%%%%%%%%%%%%%%%%%%%%%%%%%%%%%%%%%%%%%
% Semiconductor Parameters          %
%%%%%%%%%%%%%%%%%%%%%%%%%%%%%%%%%%%%%
eV = 0.1;                     % Activation Energy
K = 8.617385e-5;              % Boltzman's Constant
B1 = eV/K;                    % Activation Energy / Boltzman's Constant
C1 = 1E6;                     % Model parameter(initial lifetime?)
T = 25:5:150;                 % Stress (temperature)
V = T+273;                    % Temperature in Kelvin
cT = (1/(273+25))-(1./V);     % Change in temperature(from ambient)
L1 = C1*exp(-B1.*cT);         % Arrhenius Model for Semiconductor

%%%%%%%%%%%%%%%%%%%%%%%%%%%%%%%%%%%%%
% Winding Insulation Parameters     %
%%%%%%%%%%%%%%%%%%%%%%%%%%%%%%%%%%%%%
C2 = 10E4;                    % Initial Lifetime
Ta = 25;                      % Ambient Temperature
cT = (1/(273+25))-(1./V);     % Change in temperature(from ambient)
L2 = C2*exp(-B1.*cT);         % Arrhenius Model for Insulation

%%%%%%%%%%%%%%%%%%%%%%%%%%%%%%%%%%%%%
% Bearing Parameters                %
%%%%%%%%%%%%%%%%%%%%%%%%%%%%%%%%%%%%%
```

```
C3 = 10E4;                          % Initial Lifetime
J = 0.1:0.01:3.0;                   % Bearing Current Density
fs = 20E3;                          % Switching Frequency (20kHz)
Top = 0.50;                         % Time Operating (~50%)
W = J ;                   % Bearing Stress
L3 = C3*exp(-W);                    % Shaft Bearing Life Time

%%%%%%%%%%%%%%%%%%%%%%%%%%%%%%%%%%%%%
% Permanent Magnet Parameters       %
%%%%%%%%%%%%%%%%%%%%%%%%%%%%%%%%%%%%%
C4 = 1E6;                          % Initial Lifetime
P = T * 0.011;                      % Bearing Stress
L4 = C4*exp(-P);                    % Permanent Magnet Life Time

%%%%%%%%%%%%%%%%%%%%%%%%%%%%%%%%%%%%%
% Determine Normal Life Time        %
%%%%%%%%%%%%%%%%%%%%%%%%%%%%%%%%%%%%%
%%%%%%%%%%%%%%%%%%%%%%%%%%%%%%%%%%%%%
% Semiconductor Calculations        %
%%%%%%%%%%%%%%%%%%%%%%%%%%%%%%%%%%%%%
semi_normal_fr = 1/C1;                   % Semiconductor Failure Rate

%%%%%%%%%%%%%%%%%%%%%%%%%%%%%%%%%%%%%
% Winding Insulation Calculations   %
%%%%%%%%%%%%%%%%%%%%%%%%%%%%%%%%%%%%%
ins_normal_fr = 1/C2;                   % Winding Insulation Failure Rate

%%%%%%%%%%%%%%%%%%%%%%%%%%%%%%%%%%%%%
% Shaft Bearing Calculations        %
%%%%%%%%%%%%%%%%%%%%%%%%%%%%%%%%%%%%%
bear_normal_fr = 1/C3;                  % Shaft Bearing Failure Rate

%%%%%%%%%%%%%%%%%%%%%%%%%%%%%%%%%%%%%
% Permanent Magnet Calculations     %
%%%%%%%%%%%%%%%%%%%%%%%%%%%%%%%%%%%%%
pm_normal_fr = 1/C4;                   % Permanent Magnet Failure Rate

% Total Failure Rate
normal_fr = semi_normal_fr + ins_normal_fr + bear_normal_fr +
pm_normal_fr;

MTBF_system_normal = 1/normal_fr;      % System MTBF

MTBF_component_normal =
[1/semi_normal_fr;1/ins_normal_fr;1/pm_normal_fr;1/bear_normal_fr];
```

```
%%%%%%%%%%%%%%%%%%%%%%%%%%%%%%%%%%%%%%%%%%%%%%%%%%%%%%
% Determine Post Fault Life Time                      %
% Center Tapped DC-bus Operation (Reduced Operation)  %
%%%%%%%%%%%%%%%%%%%%%%%%%%%%%%%%%%%%%%%%%%%%%%%%%%%%%%
%%%%%%%%%%%%%%%%%%%%%%%%%%%%%%%%%%%%%
% Semiconductor Calculations        %
%%%%%%%%%%%%%%%%%%%%%%%%%%%%%%%%%%%%%
theta_ja = 62;           % Thermal Resistance of MOSFET packaging
Pd1 = 0.57;              % Average Power Dissipated (Chap 7 Eqn 7.1)
Tj = Ta + Pd1*theta_ja;   % Junction Temperature

% Thermal Stress as Function of Junction Temperature (Kelvin)
V = Tj+273; cT = (1/(273+25))-(1/V);
L1_AF = C1*exp(-B1.*cT);  % Semiconductor Life Time After Fault
semi_reduced_fr= 1/L1_AF;     % Semiconductor Failure Rate After Fault

%%%%%%%%%%%%%%%%%%%%%%%%%%%%%%%%%%%%%
% Winding Insulation Calculations   %
%%%%%%%%%%%%%%%%%%%%%%%%%%%%%%%%%%%%%
T_winding_af_1 = Ta*(2);       % Winding Temperature Rise After Fault
% Change in temperature from ambient to actual temperature
cT  = (1/(273+25))-(1./(273+T_winding_af_1));
L2_AF = C2*exp(-B1.*cT);     % Winding Insulation Life Time After Fault
ins_reduced_fr = 1/L2_AF;         % Winding Insulation Failure Rate After Fault

%%%%%%%%%%%%%%%%%%%%%%%%%%%%%%%%%%%%%
% Shaft Bearing Calculations        %
%%%%%%%%%%%%%%%%%%%%%%%%%%%%%%%%%%%%%
J = 1.0*sqrt(3);                            % Bearing Current Density
W2 = J;                           % Bearing Stress
L3_AF = C3*exp(-W2);                         % Shaft Bearing Life Time
bear_reduced_fr = 1/L3_AF;                      % Shaft Bearing Failure Rate

%%%%%%%%%%%%%%%%%%%%%%%%%%%%%%%%%%%%%
% Permanent Magnet Calculations     %
%%%%%%%%%%%%%%%%%%%%%%%%%%%%%%%%%%%%%
P = T_winding_af_1 * 0.011;                  % PM Stress
L4_AF = C4*exp(-P);                         % Permanent Magnet Life Time
pm_reduced_fr = 1/L4_AF;                        % Permanent Magnet Failure Rate

% System Failure Rate
reduced_fr = semi_reduced_fr + ins_reduced_fr + bear_reduced_fr +
pm_reduced_fr;
```

```
% System MTBF
MTBF_system_reduced = 1/normal_fr + 1/reduced_fr;

MTBF_component_reduced =
[1/semi_reduced_fr;1/ins_reduced_fr;1/pm_reduced_fr;1/bear_reduced_fr];

%%%%%%%%%%%%%%%%%%%%%%%%%%%%%%%%%%%%%
% Determine Post Fault Life Time    %
% Redundant Hardware Operation      %
%%%%%%%%%%%%%%%%%%%%%%%%%%%%%%%%%%%%%
%%%%%%%%%%%%%%%%%%%%%%%%%%%%%%%%%%%%%
% Semiconductor Calculations        %
%%%%%%%%%%%%%%%%%%%%%%%%%%%%%%%%%%%%%
theta_ja = 62;              % Thermal Resistance of MOSFET packaging
Pd = 1.0                    % Average Power Dissipated (Chap 7 Eqn 7.16)
Tj = Ta + Pd*theta_ja;      % Junction Temperature
V = Tj+273;  % Thermal Stress as Function of Junction Temperature (Kelvin)
cT = (1/(273+25))-(1./V);
L1_AF2 = C1*exp(-B1.*cT);    % Semiconductor Life Time After Fault
semi_redundant_fr = 1/L1_AF2;      % Semiconductor Failure Rate After Fault

%%%%%%%%%%%%%%%%%%%%%%%%%%%%%%%%%%%%%
% Winding Insulation Calculations   %
%%%%%%%%%%%%%%%%%%%%%%%%%%%%%%%%%%%%%
T_winding_af2 = Ta*(6);     % Winding Temperature Rise After Fault
% Change in temperature from ambient to actual temperature
cT = (1/(273+25))-(1./(273+T_winding_af2));
L2_AF2 = C2*exp(-B1.*cT); % Winding Insulation Life Time After Fault
ins_redundant_fr = 1/L2_AF2;    % Winding Insulation Failure Rate After Fault

%%%%%%%%%%%%%%%%%%%%%%%%%%%%%%%%%%%%%
% Shaft Bearing Calculations        %
%%%%%%%%%%%%%%%%%%%%%%%%%%%%%%%%%%%%%
J = 1.0;                                % Bearing Current Density
W3 = J;                             % Bearing Current Stress
L3_AF2 = C3*exp(-W3);                    % Shaft Bearing Life Time
bear_redundant_fr = 1/C3;                 % Shaft Bearing Failure Rate

%%%%%%%%%%%%%%%%%%%%%%%%%%%%%%%%%%%%%
% Permanent Magnet Calculations     %
%%%%%%%%%%%%%%%%%%%%%%%%%%%%%%%%%%%%%
P = T_winding_af2 * 0.011;              % Bearing Stress
L4_AF2 = C4*exp(-P);                    % Permanent Magnet Life Time
pm_redundant_fr = 1/L4_AF2;                   % Permanent Magnet Failure Rate
```

```
% System Failure Rate
redundant_fr = semi_redundant_fr + ins_redundant_fr +
bear_redundant_fr + pm_redundant_fr;

% System MTBF
MTBF_system_redundant = 1/normal_fr + 1/redundant_fr;
MTBF_component_redundant =
[1/semi_redundant_fr;1/ins_redundant_fr;1/pm_redundant_fr;1/bear_redundant_fr];

%Output Component Failure Rates
FR_component_normal =
[semi_normal_fr;ins_normal_fr;pm_normal_fr;bear_normal_fr];
FR_component_reduced =
[semi_reduced_fr;ins_reduced_fr;pm_reduced_fr;bear_reduced_fr];
FR_component_redundant =
[semi_redundant_fr;ins_redundant_fr;pm_redundant_fr;bear_redundant_fr];
FR_component = [FR_component_normal FR_component_reduced
FR_component_redundant]

format bank;
% Output System MTBF
MTBF_COMP=[MTBF_component_normal MTBF_component_reduced
MTBF_component_redundant] MTBF_SYS=[MTBF_system_normal
MTBF_system_reduced MTBF_system_redundant]

% Fault 1 Percent Error
perror_1 = 100*(MTBF_system_reduced  -
MTBF_system_normal)/MTBF_system_normal
% Fault 2 Percent Error
perror_2 = 100*(MTBF_system_redundant -
MTBF_system_normal)/MTBF_system_normal
```

BIBLIOGRAPHY

BIBLIOGRAPHY

[BBZZ03] N. Bianchi, S. Bolognani, M. Zigliotto, and M. Zordan. Innovative Remedial Strategies for Inverter Faults in IPM Synchronous Motor Drives. *IEEE International Transaction on Energy Conversion*, 18(2):306–312, June 2003.

[BG01] J.V. Bukowski and W.M. Goble. Defining Mean Time-to-Failure in a Particular Failure-State for Multi-Failure-State Systems. *IEEE Transactions on Reliability*, pages 221–228, June 2001.

[CL98] S. Chen and T.A. Lipo. Circulating Type Motor Bearing Current in Inverter Drives. *IEEE Industrial Applications Magazine*, pages 32–38, January/February 1998.

[DG66] G.W.A. Dummer and N.B. Griffin. *Electronics Reliability-Calculation and Design.* Pergamon Press, Ltd., 1966.

[JMH96] A.G. Jack, B.C. Mecrow, and J.A. Haylock. A Comparative Study of Permanent Magnet and Switched Reluctance Motors for High-Performance Fault-Tolerant Applications. *IEEE International Transaction on Industry Applications*, pages 889–895, July/August 1996.

[Kra99] A. Krautstrunk. Remedial Strategy for a Permanent Magnet Synchronous Motor Drive. *European Power Electronics and Drives Association.*, April 1999.

[MAOR03] P.H. Mellor, T.J. Allen, R. Ong, and Z. Rahma. Faulted Behavior of Permanent Magnet Electric Vehicle Traction Drives. In *IEEE International Electric Machines and Drives Conference*, pages 554–558, June 2003.

[MG98] D. Macdonald and W. Gray. A Practical Guide to Understanding Bearing Damage Related to PWM Drives. pages 159–165. Pulp and Paper Industry Technical Conference, June 21–26 1998.

[Mil89] T.J.E. Miller. *Brushless Permanent-Magnet and Reluctance Motor Drives.* Oxford Science Publications, 1989.

[MJHC96] B.C. Mecrow, A.G. Jack, J.A. Haylock, and J. Coles. Fault-tolerant Permanent Magnet of Machine Drives. *IEE Proceedings Electrical Power Applications*, pages 437–442, November 1996.

[MMS02] G.C. Montanari, G. Mazzanti, and L. Simoni. Progress in Electrothermal Life Modeling of Electrical Insulation during the Last Decades. *IEEE Transactions on Dielectrics and Electrical Insulation*, pages 730–745, October 2002.

[Mon00] G.C. Montanari. Insulation aging and life models. *IEEE Industrial Applications Magazine*, pages 1–7, January 2000.

[Mue04] A. Muetze. *Bearing Currents in Inverter-Fed AC-Motors.* Shaker Verlag., 2004.

[Nat04] National Semiconductor Corporation. Reliability Programs., Nov 2004. http://www.national.com/quality/reliability_programs.html.

[PR02] P.V.N. Prasad and K.R.M. Rao. Reliability Models of Repairable Systems Considering the Effect of Operating Conditions. *IEEE International Reliability and Maintainability Symposium Proceedings, Annual*, pages 503–510, January 2002.

[Rel04a] Reliasoft Corporation. Arrjenius Relationship Introduction. Sept 2004. http://www.weibull.com/AccelTestWeb/arrhenius_relationship_introduction.htm.

[Rel04b] Reliasoft Corporation. What is Accelerated Life Testing? Dec 2004. http://www.weibull.com/AccelTestWeb/what_is_accelerated_life_testing_.htm.

[WLJS03] B.A. Welchko, T.A. Lipo, T.M. Jahns, and S.E. Schulz. Fault Tolerant Three-phase AC Motor Drive Topologies; a Comparison of Features, Cost, and Limitations. In *IEEE International Electric Machines and Drives Conference*, pages 539–546, June 2003.